1995

Development and testing of a VTOL UAV

Cibula, Andrew Lee.

Monterey, California. Naval Postgraduate School

NAVAL POSTGRADUATE SCHOOL
MONTEREY, CALIFORNIA

THESIS

DEVELOPMENT AND TESTING OF A VTOL UAV

by

Andrew Lee Cibula

June 1995

Thesis Advisor: Richard M. Howard

Approved for public release; distribution is unlimited

DISCLAIMER NOTICE

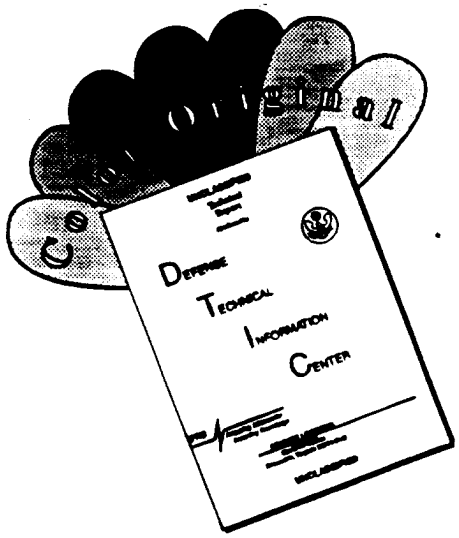

THIS DOCUMENT IS BEST QUALITY AVAILABLE. THE COPY FURNISHED TO DTIC CONTAINED A SIGNIFICANT NUMBER OF COLOR PAGES WHICH DO NOT REPRODUCE LEGIBLY ON BLACK AND WHITE MICROFICHE.

1REPORT DOCUMENTATION PAGE

Form Approved OMB Np. 0704-0188

1. AGENCY USE ONLY *(Leave blank)*	2. REPORT DATE June 1995	3. REPORT TYPE AND DATES COVERED Master's Thesis

4. TITLE AND SUBTITLE DEVELOPMENT AND TESTING OF A VTOL UAV

5. FUNDING NUMBERS

6. AUTHOR(S) Cibula, Andrew L.

7. PERFORMING ORGANIZATION NAME(S) AND ADDRESS(ES)
Naval Postgraduate School
Monterey CA 93943-5000

8. PERFORMING ORGANIZATION REPORT NUMBER

9. SPONSORING/MONITORING AGENCY NAME(S) AND ADDRESS(ES)

10. SPONSORING/MONITORING AGENCY REPORT NUMBER

11. SUPPLEMENTARY NOTES The views expressed in this thesis are those of the author and do not reflect the official policy or position of the Department of Defense or the U.S. Government.

12a. DISTRIBUTION/AVAILABILITY STATEMENT
Approved for public release; distribution is unlimited.

12b. DISTRIBUTION CODE

13. ABSTRACT *(maximum 200 words)*

The purpose of this project was to develop a testing platform to prepare a Vertical Takeoff and Landing Unmanned Air Vehicle (VTOL UAV) for fully independent flight tests. Other preparations for flight included extensive engine thrust and endurance testing to fully evaluate the capabilities of the engine used. Also, redesign of the fuel system allowed more efficient use of the fuel onboard. Commands for thrust and steering data were transmitted to the VTOL UAV via an RF uplink while UAV attitude and positional data were returned by means of an umbilical cable. Throttle settings, vane control, and a kill switch were incorporated in the RF uplink. The testing platform was developed to allow the VTOL UAV to hover in a confined area with limited movement in order to accurately monitor the effectiveness of the flight control system. In this regard, the vehicle was allowed only several feet of movement in any direction by fastening it in an aluminum cubical frame designed for this purpose. This thesis was carried out in conjunction with another flight control project and was aimed at providing the vehicle a platform in which to operate within a constricted area.

14. SUBJECT TERMS AROD, Archytas, Unmanned Air Vehicle (UAV), Design, VTOL

15. NUMBER OF PAGES 100

16. PRICE CODE

17. SECURITY CLASSIFICATION OF REPORT	18. SECURITY CLASSIFICATION OF THIS PAGE	19. SECURITY CLASSIFICATION OF ABSTRACT	20. LIMITATION OF ABSTRACT
Unclassified	Unclassified	Unclassified	UL

NSN 7540-01-280-5500 Standard Form 298 (Rev. 2-89)

Prescribed by ANSI Std. 239-18

Approved for public release; distribution is unlimited

DEVELOPMENT AND TESTING OF A VTOL UAV

Andrew L. Cibula
Lieutenant, United States Navy
B.S., Marquette University, 1987

Submitted in partial fulfillment of the
requirements for the degree of

MASTER OF SCIENCE IN AERONAUTICAL ENGINEERING

from the

NAVAL POSTGRADUATE SCHOOL
June 1995

Author: [redacted]
Andrew L. Cibula

Approved by: [redacted]
Richard M. Howard, Thesis Advisor

[redacted]
Garth V. Hobson, Second Reader

[redacted]
Daniel J. Collins, Chairman

Department of Aeronautics and Astronautics

ABSTRACT

The purpose of this project was to develop a testing platform to prepare a Vertical Takeoff and Landing Unmanned Air Vehicle (VTOL UAV) for fully independent flight tests. Other preparations for flight included extensive engine thrust and endurance testing to fully evaluate the capabilities of the engine used. Also, redesign of the fuel system allowed more efficient use of the fuel onboard. Commands for thrust and steering data were transmitted to the VTOL UAV via an RF uplink while UAV attitude and positional data were returned by means of an umbilical cable. Throttle settings, vane control, and a kill switch were incorporated in the RF uplink. The testing platform was developed to allow the VTOL UAV to hover in a confined area with limited movement in order to accurately monitor the effectiveness of the flight control system. In this regard, the vehicle was allowed only several feet of movement in any direction by fastening it in an aluminum cubical frame designed for this purpose. This thesis was carried out in conjunction with another flight control project and was aimed at providing the vehicle a platform in which to operate within a constricted area.

TABLE OF CONTENTS

ACKNOWLEDGMENTS

There are numerous people involved with this project to whom I owe a great deal of thanks. It was only due to their guidance, cooperation and patience that I was able to complete it. A special thanks to Don Meeks for his knowledge and help in the mechanical aspects of this thesis. Also, thanks to Jeff Test who provided his services and instruction on the majority of the electrical work. Without the tireless patience of these two, this project would have never happened.

Also, my sincere appreciation to Dr. Isaac Kaminer whose cooperation enabled a smoother completion of my thesis. Next, it was an honor to work with my advisor, Dr. Richard Howard, whose leadership and encouragement were instrumental in the completion of this project. It was a heartfelt pleasure to have the opportunity to work for him.

Finally, I would like to thank both Jennifer and John. Jennifer for her continued understanding and assurances, and John, whose endless pursuit of an engine allowed me to advance my cause considerably.

I. INTRODUCTION

A. BACKGROUND

The first actual use of an Unmanned Air Vehicle (UAV) in wartime came about when an aerial camera was mounted to the airframe of a Ryan Q-2C Firebee target drone in 1960 [Ref. 1]. The role of this vehicle was photographic surveillance and reconnaissance. Since that time, UAVs have been pressed into a myriad of roles including weather monitoring, communications relay, over-the-horizon targeting, and battle damage assessment. Early in their development, the primary advantage of these vehicles was realized as an inexpensive UAV could be sent into a hostile environment without risking an aircrew or costly aircraft.

During Operation Desert Storm, the Remotely Piloted Vehicle (RPV) proved valuable for information gathering and surveillance purposes. However, limitations in the abilities of these vehicles were noted. For example, the Pioneer program was successful for surveillance, but the need for extended support such as a groomed runway limited their usefulness [Ref. 2]. Limitations such as this, were the impetus for the development of UAVs that were multi-mission capable and required limited support. Additionally, because of UAV successes in the gulf, a push to further develop the short-range UAV as an integrated force in battle was initiated [Ref. 3].

Unfortunately, obstacles such as budget cuts arose, which stymied the continued development and testing of reconnaissance vehicles in general, and UAV programs specifically. Because of these cuts, the armed services were forced to choose between

large weapon system programs or the UAV, with UAV budgets taking the cut. Within the last year, the Defense Department downsized or eliminated several reconnaissance programs, including the Air Force/ Navy Advance Tactical Airborne and Reconnaissance System (ATARS) [Ref. 4]. Cuts such as these can degrade future reconnaissance capabilities for the services by creating a gap in active UAV programs. However, the Naval Postgraduate School UAV Flight Research Laboratory (NPS UAV FRL) attempts to fill this void by resurrecting airframes from canceled UAV programs to advance UAV technologies. This mission is the motivation for this thesis.

B. UAV WORK AT NPS

This thesis outlines the work completed on the Archytas Ducted Fan (ADF) UAV. The Archytas program is a continuation of several projects started earlier at NPS involving the Airborne Remotely Operated Device (AROD) and the Aquila airframes. The ADF project is divided into two parts, with the first addressing the platform's flight control system [Ref. 5] and the second covering the testing and evaluation of the ADF. This thesis entails work on the testing and evaluation section of this project.

The Naval Postgraduate School UAV FRL recognizes the need for the UAV in military strategy. The original Archytas Tailsitter was designed to overcome the limitations of the Pioneer's need for extensive support. It was designed to take-off vertically, transition to horizontal flight, fly its mission and land again vertically. The ADF, on the other hand, responded to the need for a UAV, under RF control, in both a hover and at slow speeds, to carry a payload of instruments such as cameras,

spectroradiometers, and light sensors [Ref. 6]. The missions required that a UAV take off and land on the beach and cruise at an altitude between 175 and 200 feet at five knots.

The ADF originally began as an AROD airframe but has undergone significant changes at NPS. Those changes, some of which are documented in this thesis, include:

- Redesigned flight control system incorporating an Inertial Measurement Unit and both an RF uplink and downlink.
- Addition of antennas and receivers that control the throttle, vane servos, and kill switch.
- Structural changes such as fuel system and test stand attachments.

In addition to changes to the vehicle, engine testing and construction of a hover test stand were completed. The goals of the vehicle tests were to:

- Determine engine thrust and engine speed (rpm) data.
- Determine the reliability of the flight control wiring during engine operation.
- Test the flight control system in a constrained environment by hovering the vehicle in the hover test stand.
- Use RF signals solely to operate the vehicle.

The following four chapters discuss the procedures used and the problems associated with accomplishing the above mentioned objectives.

II. BACKGROUND

A. GENERAL INFORMATION ON UAVS

After the use of reconnaissance vehicles had been realized, the Department of Defense reinitiated its interest in Unmanned Air Vehicles. The emphasis was placed on endurance, stealth, and limited support [Ref. 7]. Furthermore, it has been predicted that 1995 will be the year that the military learns to fully integrate reconnaissance UAVs in military uses. This has already been demonstrated by the use of UAVs as information gatherers in Bosnia [Ref. 8]. This new push for UAVs provided the impetus for the Naval Postgraduate School to continue its research on Unmanned Air Vehicles.

The work done at the Naval Postgraduate School was conducted towards developing a vehicle that could operate in a multitude of environments with limited support. Previous work done at the UAV FRL has concentrated on close range UAVs which generally operate in the 30-50 km range [Ref. 9]. These UAVs would ideally serve as the eyes and ears for military units, such as a Marine Expeditionary Unit, with limited available intelligence. The UAV FRL has previously worked with assets from several canceled programs such as the AROD, Pioneer and Aquila, which could be modified and improved to advance the state-of-the art in UAV technologies.

B. UAV PROGRAMS AT NPS

1. AROD

The Airborne Remotely Operated Device (AROD) was created by engineers at Sandia National Laboratories in Albuquerque, New Mexico to provide quick battlefield reconnaissance without risking lives [Ref. 10]. It was designed to be controlled via fiber optic cable from a suitcase-sized ground unit (Figure 1).

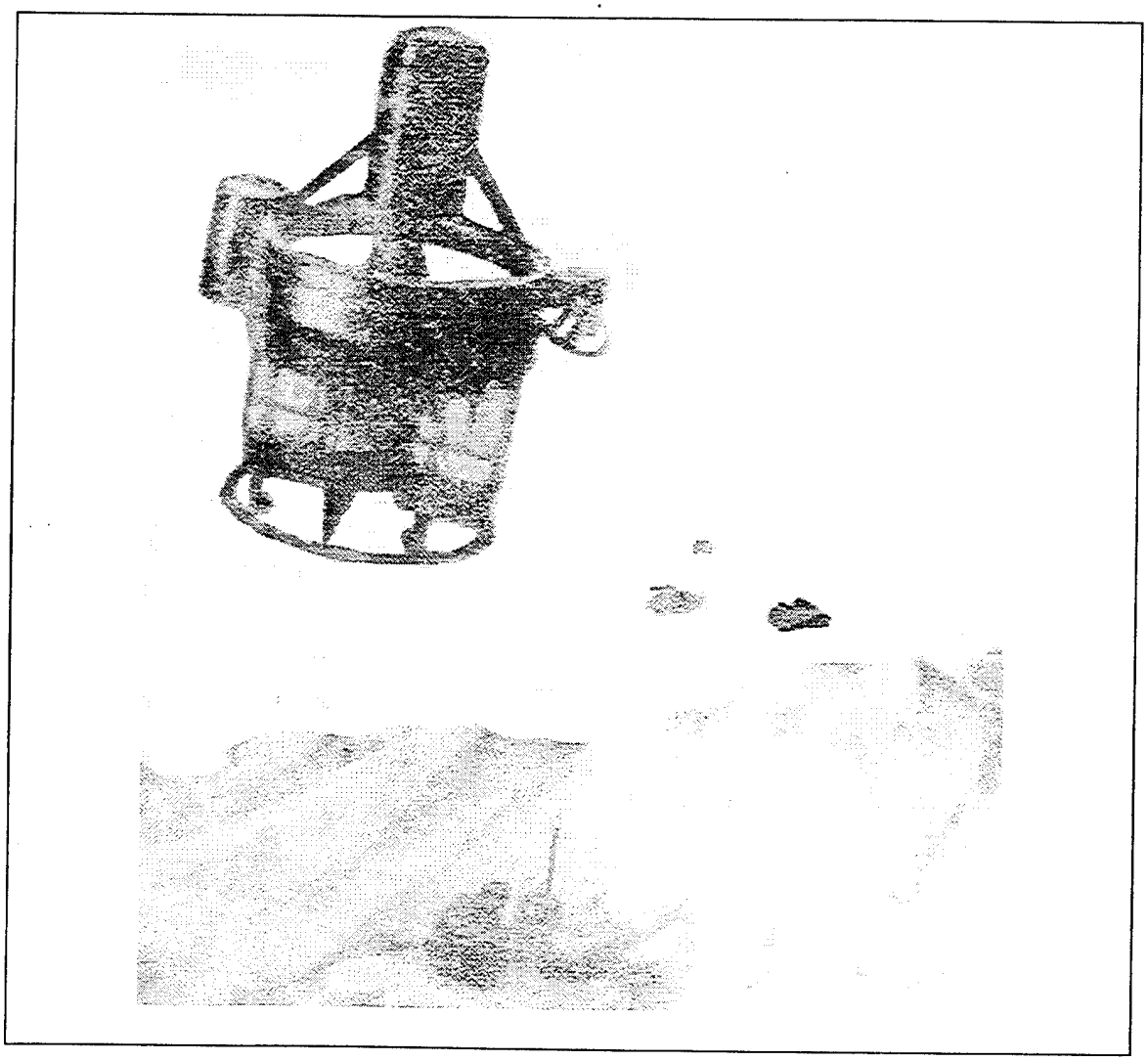

Figure 1 - AROD Mission Profile

The vehicle was to carry two onboard cameras that fed video of terrain as well as troop movements down to a Marine unit below. The AROD weighed about 85 pounds and could operate for up to an hour at a range of 18 miles. The vehicle stayed aloft using powered lift from a ducted fan, driven by a 26-hp, 2-stroke, 2-cylinder gasoline engine. An onboard computer was required for data monitoring and control and stabilization. Four vanes at the duct exit provided directional and rotational control for the vehicle. The Naval Postgraduate School received several airframes after the U.S. Marine Corps program was canceled.

2. Pioneer

The Pioneer was a mini-RPV originally designed by the Israelis (Figure 2). The U.S. acquired a total of three Pioneer systems in 1986; two were used for shipboard purposes and a third to form a Marine based RPV platoon [Ref. 11]. The primary Navy use for the vehicle was for gunfire support, with the shipboard vehicles deployed to battleships, and launched with the help of rocket boosters and recovered using large nets. During the Gulf War, the Marine platoon used the Pioneer extensively for gunfire

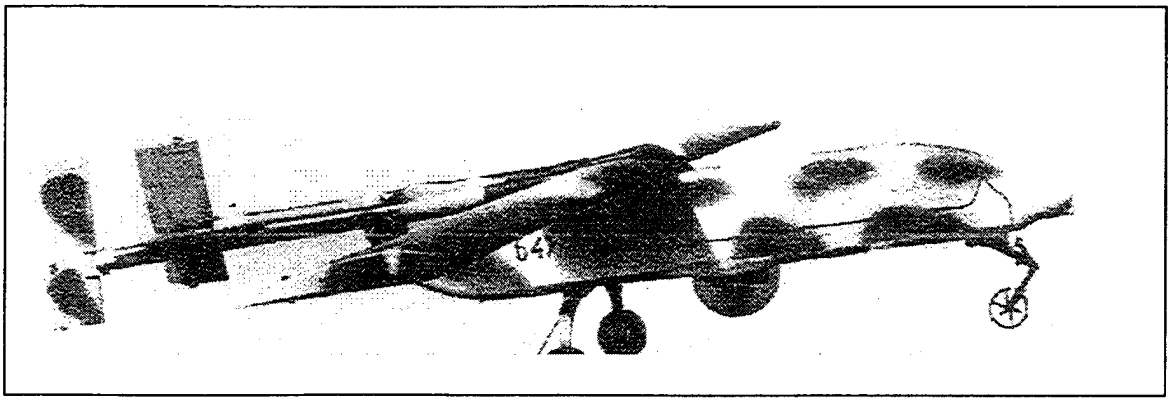

Figure 2 - Pioneer UAV

support and reconnaissance with successful results. However, as mentioned earlier, paved runways were required for the Pioneer to operate, so its use was limited. The UAV FRL acquired a one-half size model of the Pioneer and used it at length for research in UAV capabilities and parameter identification, in order to provide an aerodynamic model for training purposes using simulation [Ref. 12].

3. Aquila

The Aquila was a short range RPV that was in use by the U.S. Army for aerial reconnaissance, real time target acquisition, first round fire for effect, artillery adjustment, and laser target designation. The program was begun in 1975 and by 1986, some 330 flights had been completed [Ref. 13]. During these flights, the Aquila was successful in locating and identifying enemy tank positions with real-time data. These positions were then targeted for artillery fire in which the enemy tanks were destroyed. One potential problem with the Aquila was the large amount of field support needed to fly the RPV (Figure 3). This need for extensive support limited its role, as was the case for the Pioneer. The Army had hoped to purchase a large number of these vehicles but the program was canceled in 1987.

NPS, however, was able to acquire several Aquila airframes. The first project undertaken by the UAV FRL was to combine the vertical takeoff and landing capabilities of the AROD with the wings of the Aquila to form the Archytas Tailsitter. A second project, which is still ongoing, is to redesign the Aquila by adding landing gear

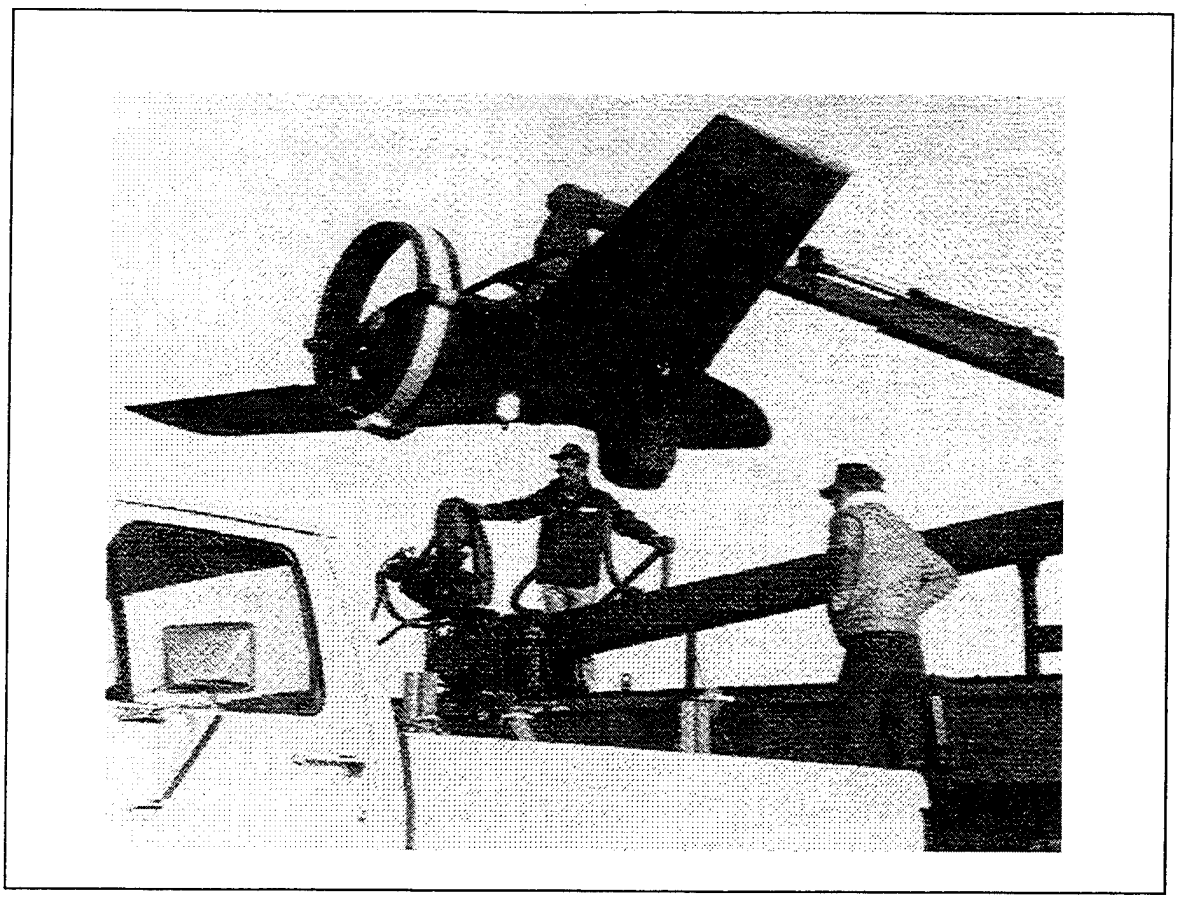

Figure 3 - Aquila With Support Vehicle

and an empennage for stability, in order to provide a suitable payload carrier [Ref. 14]. It is expected that this vehicle will be used for extensive future research.

4. Archytas Tailsitter

The Archytas Tailsitter was a program to modify the AROD into a more usable form. It was designed at the UAV FRL to combine the VTOL advantages of the AROD with the more maneuverable qualities of a fixed-wing aircraft, by combining the AROD airframe with the Aquila wings (Figure 4). The vehicle would have the capability of taking off and landing vertically and transitioning to forward flight once airborne. This

additional mobility would have alleviated the disadvantages of both the Aquila and Pioneer, by reducing the need for major support such as paved runways or lifting cranes.

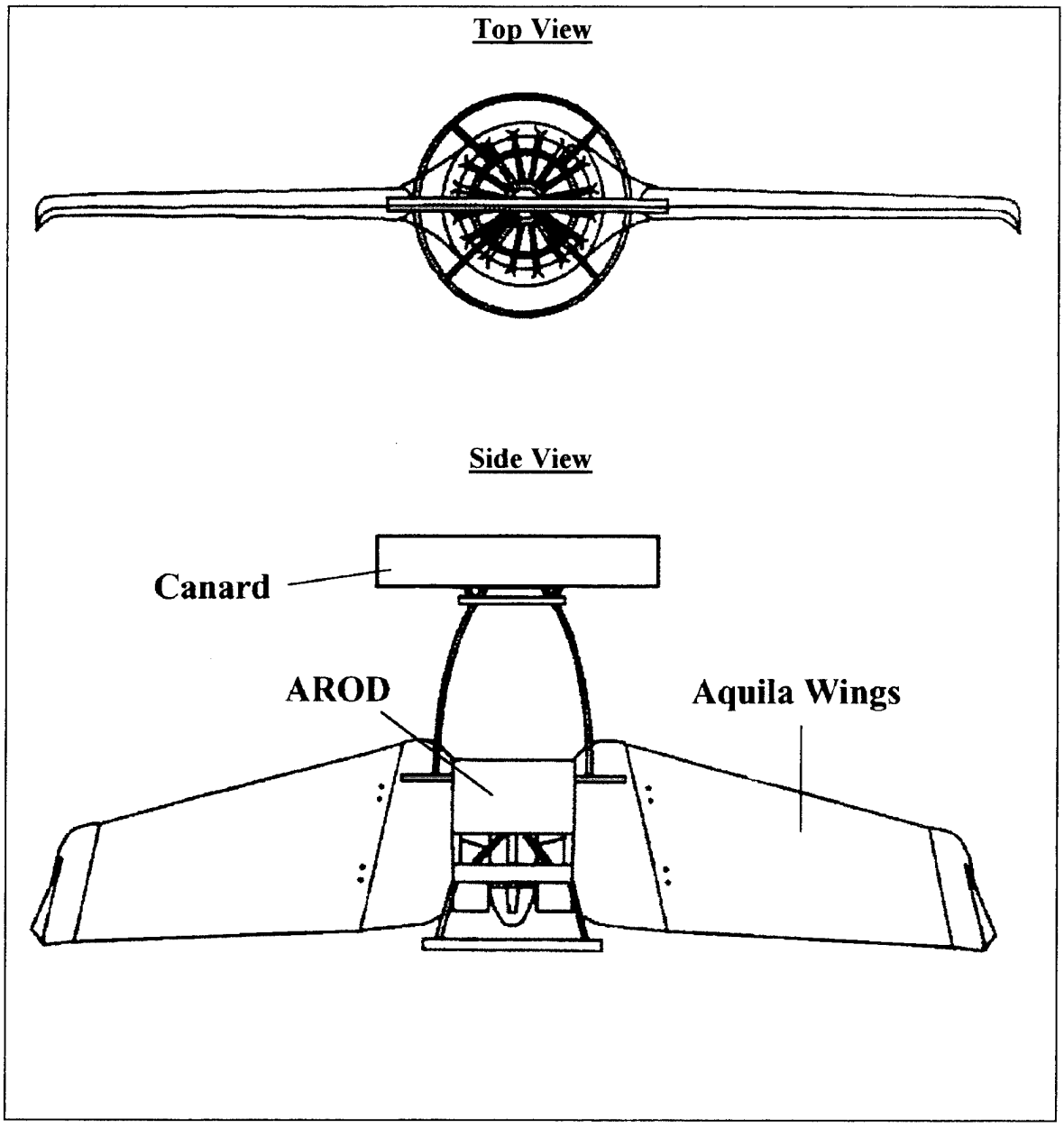

Figure 4 - Archytas Design

C. ADF CHARACTERISTICS

As mentioned earlier, the ADF is a derivative of the canceled U.S. Marine Corps project, the Airborne Remotely Operated Device (AROD). Much of the actual hardware onboard the ADF is taken directly from the AROD. The following paragraphs will describe the pertinent characteristics of both vehicles, which include the shroud or frame, the engine and its components and the control surfaces or vanes.

1. Shroud, Frame and Control Vanes

The airframe, duct, and control surfaces form the base of the ADF (Figure 5). The vehicle stands 36 inches high and is 30 inches in diameter; a complete list of physical characteristics is provided in Table 1. The shroud forms the duct which encloses

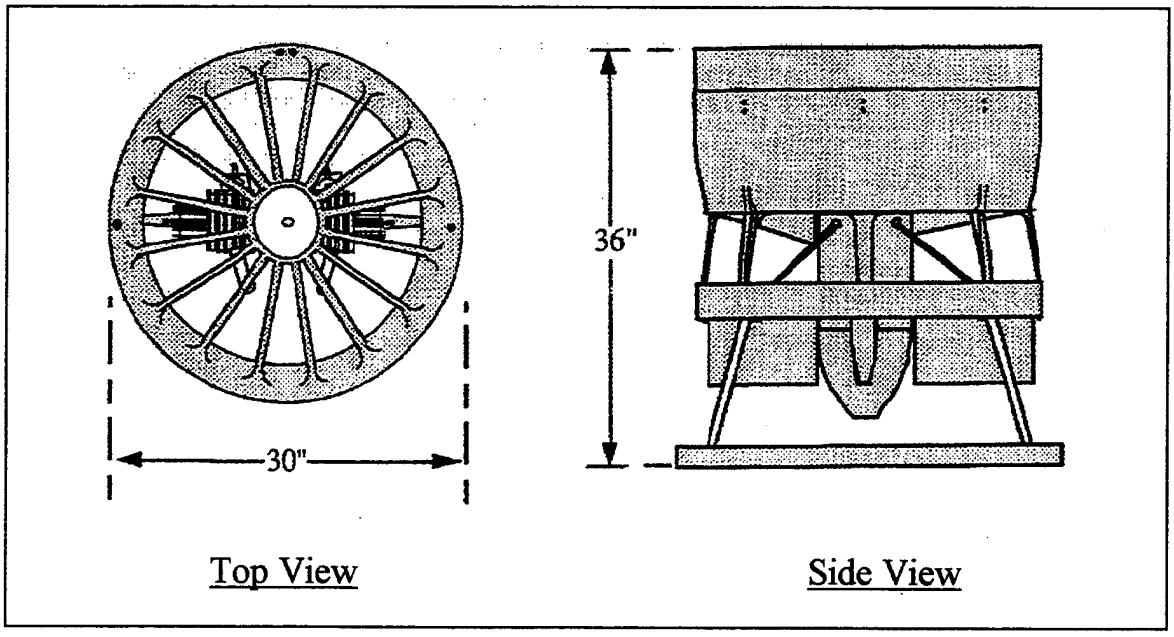

Figure 5 - AROD / ADF Frame

the propeller and also houses the fuel tank. To minimize weight, the airframe was constructed primarily of composite materials such as fiberglass, kevlar and carbon. The shroud was constructed in two parts and molded together using a plywood mount which provided support at the propeller level.

The basic frame was comprised of tubular aluminum so it could rigidly support the engine during operations. The extra support was required because of the minimal propeller tip clearance in the inlet duct. If the propeller should breach the shroud, it would also break the integrity of the fuel tank, possibly causing catastrophic failure. The engine was mounted vertically and held in place with the use of a mounting spider. Below the engine is the lower body of the vehicle. This portion of the ADF houses a majority of the electrical equipment onboard the vehicle. The lower body also contains the connection points for the control vanes which are located in the exhaust flow just underneath the engine.

Two sets of vanes are used in the vehicle to provide stability. They are in the shape of a NACA 0012 airfoil and have a six-inch chord. An aluminum skeletal frame is used for external stiffness while a foam inside provides internal rigidity. Because the pivot point of the airfoil is located at the quarter-chord, only low-torque servos are required to rotate the vanes. Small Futaba Model S34 servos were initially used to control vane deflection; however, the servos were subsequently upgraded to ensure robustness. Previous failure of the original servo system had been noted in phone conversations with Sandia personnel.

Component	Measurement
Duct Inlet Diameter	29.25 inches
Shroud Outside Diameter	30.00 inches
Height	36.00 inches
Propeller Diameter	24.00 inches
Duct Exit Diameter	26.75 inches
Inlet Area Ratio	1.219
Exit Area Ratio	1.115
Number of Blades	3
Tip Clearance	0.031 ± 0.005 inches
Engine Speed, Maximum	8000 rpm
Engine Speed, Nominal	7000 rpm
Tip Speed, Maximum	838 fpm
Tip Speed, Nominal	733 fpm

Table 1 - ADF Characteristics

2. Engine and Propeller

The engine was the sole source of power on the vehicle. It was a 2-cylinder, 2-stroke, 290 c.c. (17.4 cu in) Dynad gasoline engine which was a derivative of the

chainsaw engines developed by D. Herbrandson of the D.H. Enterprises for the Aquila program [Ref. 15]. The ADF used the modified engine which incorporated larger carburetors and was rated at 26 hp at 8000 rpm. The engine was run with short exhaust stacks and weighed 15 pounds with a power-to-weight ratio of 1.7. The engine was mounted as shown in Appendix A (Figure A.2).

The engine was a pull-start type engine which used a small cord wrapped around a cylindrical mount much like a lawnmower (Figure A.1). It required an external power source for ignition, which supplied 28V DC power initially, but once the vehicle was started, it was capable of using its own generator power to run the vehicle. An Electro-Pacific, Model 1-1152, AC electrical generator was used to generate this onboard power. The generator weighed 3-3.5 pounds and was two inches in diameter and two inches long. The generator output varied from 36 volts at 5500 rpm to 50 volts at 7500 rpm. At normal operating speeds, the generator produced about 150 Watts. Care had to be taken not to run all onboard electrical systems at idle since the power output could have been insufficient.

Engine ignition used a capacitive discharge ignition (CDI) module which simultaneously fired the engine's spark plugs. The CDI module, which was contained in a single aluminum housing, weighed about 1.2 pounds and was mounted just below the lower engine mounting plate inside the rear body. Power was supplied to the ignition circuit via the external power source or the onboard generator. A magnetic timing sensor detected a tab on the magnetic timing plate just above it and then sent the signal to the ignition circuit which activated the spark plugs. The magnetic pickup was held in position

on the upper engine mount by a single nut and could come loose due to engine vibrations. Therefore, the pickup needed to be checked periodically to ensure it was secure.

The engine drove a fixed-pitch propeller which was located within the shroud in the upper body. The propeller had three blades with a tip pitch angle of 14° which optimized thrust at maximum engine power. The three blades were made of a composite material to decrease weight and increase strength.

III. FLIGHT CONTROL SYSTEM / ELECTRICAL

A. FLIGHT CONTROL SYSTEM

The ADF operates and acts much like other hovering vehicles which means that the vehicle is an inherently unstable platform when flying. To compensate for this, the Naval Postgraduate School has developed a Stability Augmentation System (SAS), designed to provide flight worthy response to pilot commands from a remote ground station [Ref. 5]. Pilot commands are initiated by means of a joystick and sent to the C30 hardware and software located inside the 486 PC (Figure 6). The C30 is responsible for processing SAS commands and performing all necessary computations for the flight control system. The SAS uses an inertial measurement unit (IMU), which is located in the pod on top of the ADF, to monitor and detect inertial attitude, position, and movements. These signals are sent back to the C30 computer on the ground via the umbilical connector or RF downlink, where it is then converted to body, or ADF, coordinates. The initial design incorporated a umbilical cord which fed and received all information to and from the ADF (Figure 6.a), but future designs intend to incorporate an RF only uplink and downlink system (Figure 6.b)

The C30 compares the position and attitude information requested by the joystick, with the actual position and attitude information of the ADF. Next, the C30 sends the appropriate signals to the control vanes in order to adjust the ADF's position. The IMU senses the new measurements and returns them to the PC for comparison. Again, the C30

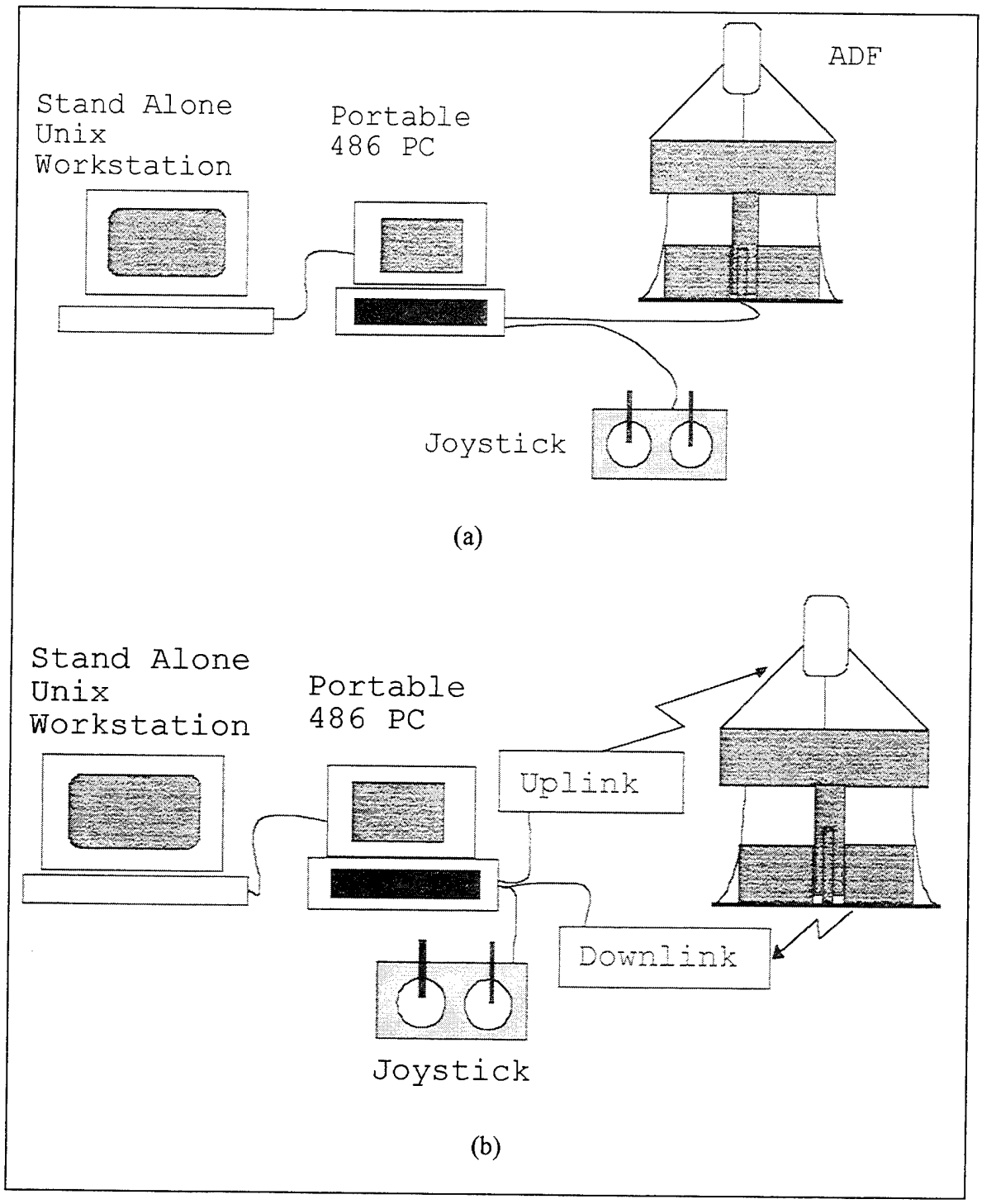

Figure 6 - Flight Control Setup

sends the corrections to the control vanes so the ADF can readjust its position. This is an iterative process and eventually the ADF's position matches the requested position within a dictated tolerance. This process closely resembles a fly-by-wire system in modern aircraft.

As a first step in creating an independent (cordless) vehicle, all uplink commands were incorporated into an RF uplink scheme. Vane positions, throttle settings, and the kill switch were initially selected as the uplink signals for the SAS; however, during the engine performance tests, only the throttle and kill switch were used. Throttle settings and the kill switch eventually remained independent of the C30 so the vehicle could be recovered in the event of a computer failure. Control vane commands were sent from the C30 up to the vehicle using interfaces in the 486 PC.

B. UPLINK

1. Transmitter / Receiver

Both the transmitter and receiver used were Futaba components used primarily for model airplane operation. The transmitter used was a Futaba PCM FP-T5SGA-P eight channel transmitter and the receiver was a Futaba PCM FP-R118GP eight channel receiver. These are shown in Appendix B, Figures B.1 and B.2 respectively. The transmitter sends one or a number of signals to the receiver where it forwards the signal to servos that control anything from landing gear to flaps.

For performance tests discussed in Chapter IV, the throttle was routed through channel three while the kill switch ran through channel five. Channel five was used for the

kill switch as it is an on-off switch. Therefore, the kill switch is either in the on or the off position whereas the throttle can be in a number of settings. The control vanes were initially tested through the transmitter but since they were computer driven, the input signal to the control vanes was sent to the ADF via hardware incorporated in the 486 PC [Ref. 5].

2. Power Supply

Power to the servos was provided from a standard 1000 mA 4.8V DC Futaba Power Pack NR-4RB battery which was attached to the shroud of the ADF. The battery first supplied power to the receiver onboard the vehicle and then the power was rerouted to the terminal board (TBS3) and finally to the servos (Figure 7). The system originally was designed to supply power from the ADF's 28V DC generator to be converted to 5V DC. However, the +5V DC power regulators were prone to failure when the vehicle engine was run at high speeds [Ref. 16], so a battery power source was added to ensure proper servo operation.

Servos used were Futaba FP-S31S indirect-drive servos modified for servo positional feedback. The signal from the uplink drives the servo to adjust the control vanes or throttle and the individual throttle positions are returned to the C30 computer through the umbilical cord.

Once the power is connected to TBS3, it can also be routed to other equipment if necessary. One problem, however, is to ensure that the battery is fully charged and is not depleted during ADF operation. During engine tests, where the battery supplied power to

only the throttle and kill switch, all control vane servos were disconnected to avoid any power drain. In this setup, there was more than sufficient power to supply the throttle and kill switch with very little drain on the battery noted. The battery was used for four to five hours without a problem. Once the control vanes are connected however, there may be significant drain on the battery. Testing needs to be done to determine the exact life of the battery. If the battery fails inflight, catastrophic failure can occur.

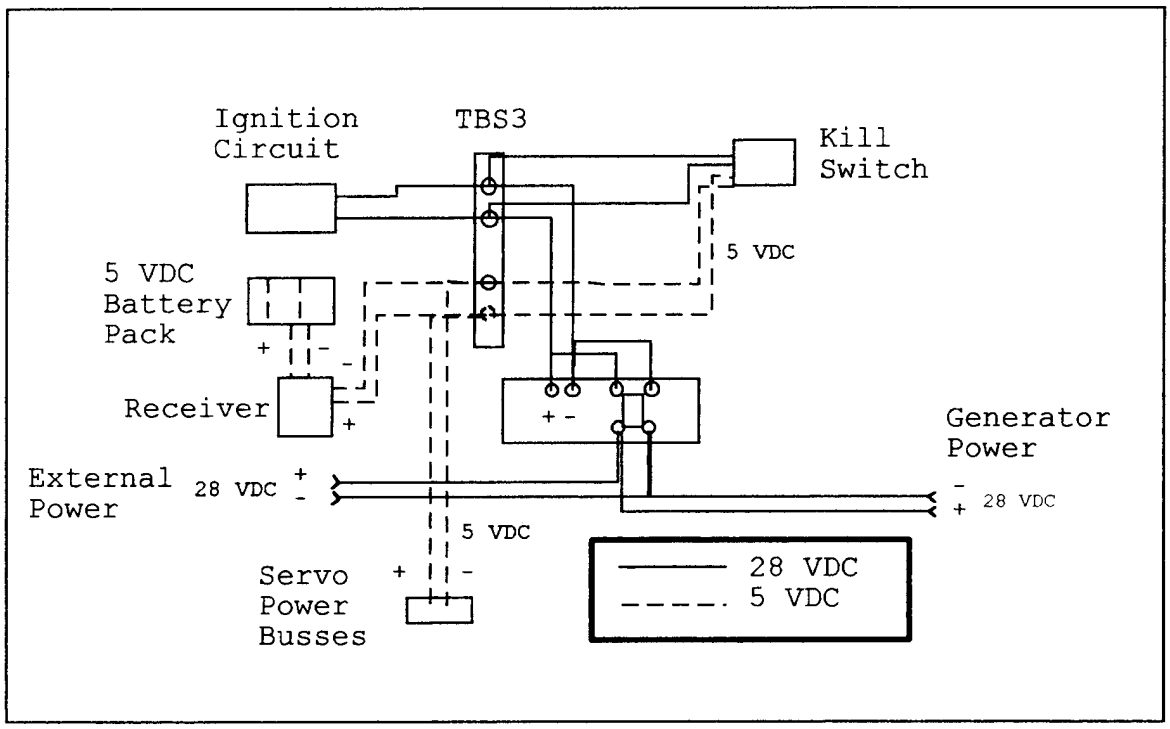

Figure 7 - Ignition and Servo Wiring

C. ADF WIRING

Aside from the servo wiring, the ignition circuits on the ADF were rewired as well. In order to start the vehicle, an external 28V DC power source needed to be

connected to the vehicle for ignition power, until the ADF's onboard generator was able to supply the appropriate power. The power supply used was connected to the main circuit board on the body of the ADF. To accomplish this, a plug was fabricated which allowed the power source to be attached and removed easily (Figure 8). The plug was hardwired into the capacitor on the circuit board. This setup allowed the external power

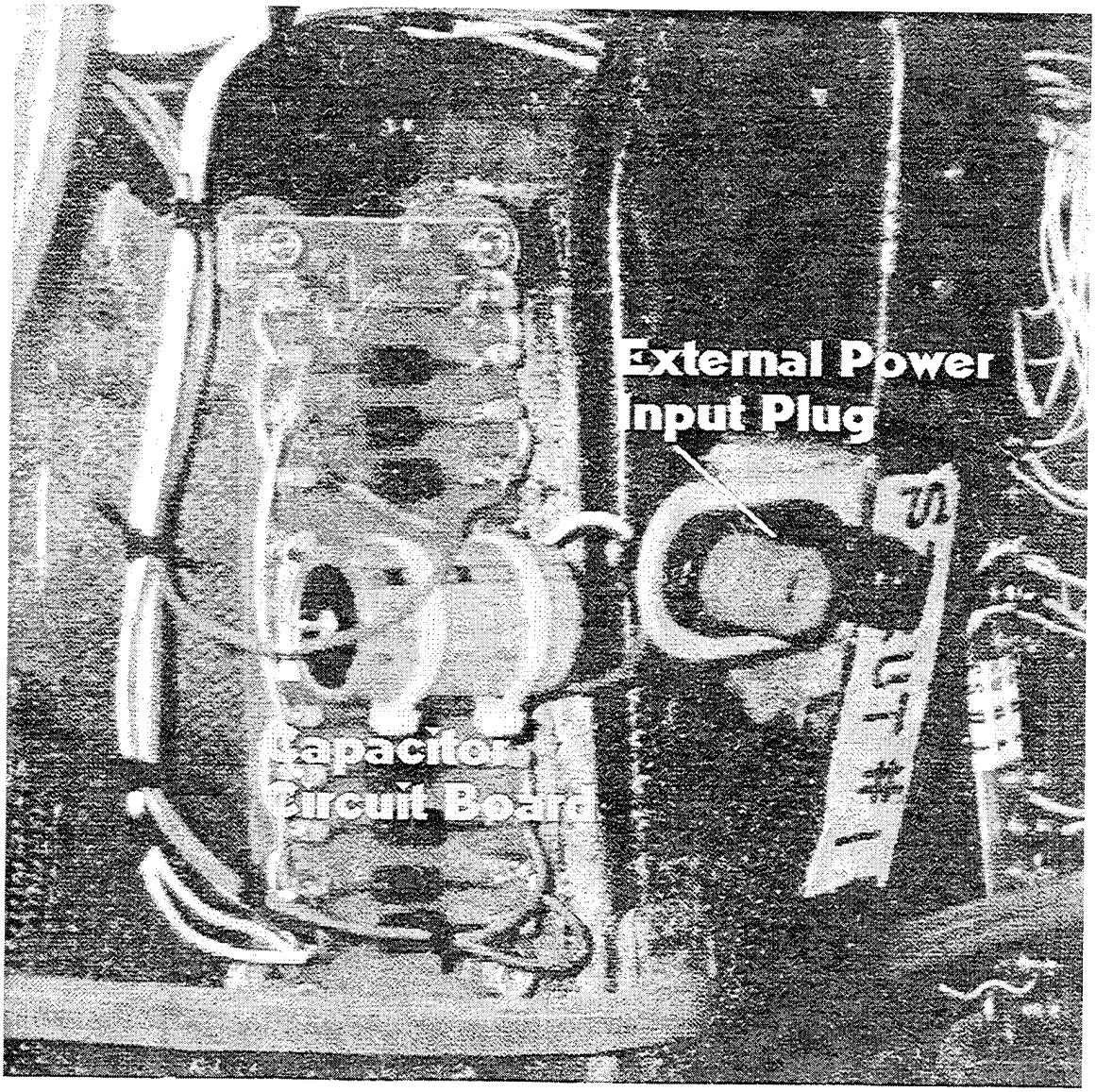

Figure 8 - External Power Supply Input

source to deliver sufficient power to the vehicle. Such a connection was necessary for flight operations, as the external power source needs to be removed quickly and easily. Once the onboard generator supplies sufficient power, external wires would only interfere with a hovering vehicle.

1. Kill Switch

The kill switch was derived from a standard Futaba servo and a microswitch. The microswitch was simply attached to the top of the servo and the connection through the

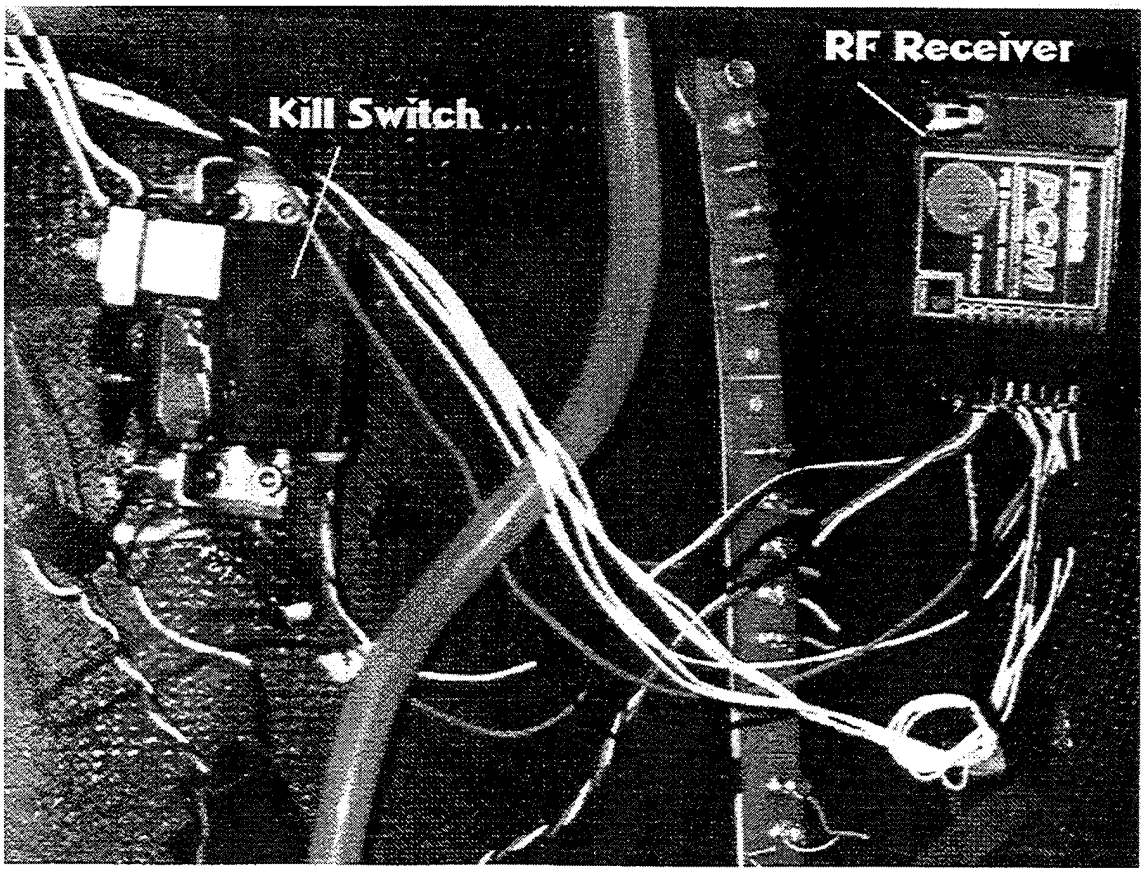

Figure 9 - Kill Switch And RF Receiver

microswitch was completed when the wheel on the servo rotated and depressed the tab on the microswitch, allowing current to flow through the microswitch (Figure 9).

Figure 7 shows the positive and negative feeds into the ignition circuit going into the kill switch. The kill switch works by completing the circuit thereby causing a short in the circuit. Originally the kill switch had the positive ignition feed run through it but was later changed to the above configuration so there would always be a continuous connection to the ignition circuit. Since the ADF had extensive vibration, a continuous connection through the microswitch could not be guaranteed; therefore, a short was used as the preferred engine shutoff method .

IV. PERFORMANCE TESTING

A. ENGINE TESTING

Engine testing was done over a period of approximately two weeks. Objectives of the tests were to:

1. Test the ignition wiring, external power supply, and engine generator power.
2. Ensure throttle and kill servos operated properly and effectively.
3. Verify engine performance at a number of throttle settings.
4. Measure thrust output and engine fuel usage at a number of rpm settings.
5. Ensure proper performance of the fuel control system.
6. Measure cylinder head and exhaust gas temperatures.
7. Verify reliable engine performance to prepare the vehicle for limited hover testing.

After the wiring was completed for the ignition system, the ADF was secured into a thrust test stand [Ref. 17]. The external power supply was attached and initial engine runups were conducted in order to check the reliability of both the throttle and kill servos and to ensure the engine could be controlled properly. Once the kill switch and throttle proved effective, the engine was again run up but this time the external power supply was turned off to see if the engine's generator could supply the proper power to the vehicle. The engine rpm was then varied from idle to maximum rpm to ensure the generator operated properly at all throttle settings. Next, the engine's rpm was calibrated to ensure the correct rpm could be read from the ADF.

1. Tachometer Calibration

The tachometer output was returned from the CDI magnetic pickup through the ignition circuit. This output was assumed to be in the form of a 'spike' that could be read either from an oscilloscope or a frequency counter. Three methods to determine RPM output were tested and compared to determine which was most accurate. The first method used a Tektronix 2245A 100 Mhz oscilloscope, where the 'spikes' could be seen and the time between them manually measured (Figure 10). The second method used

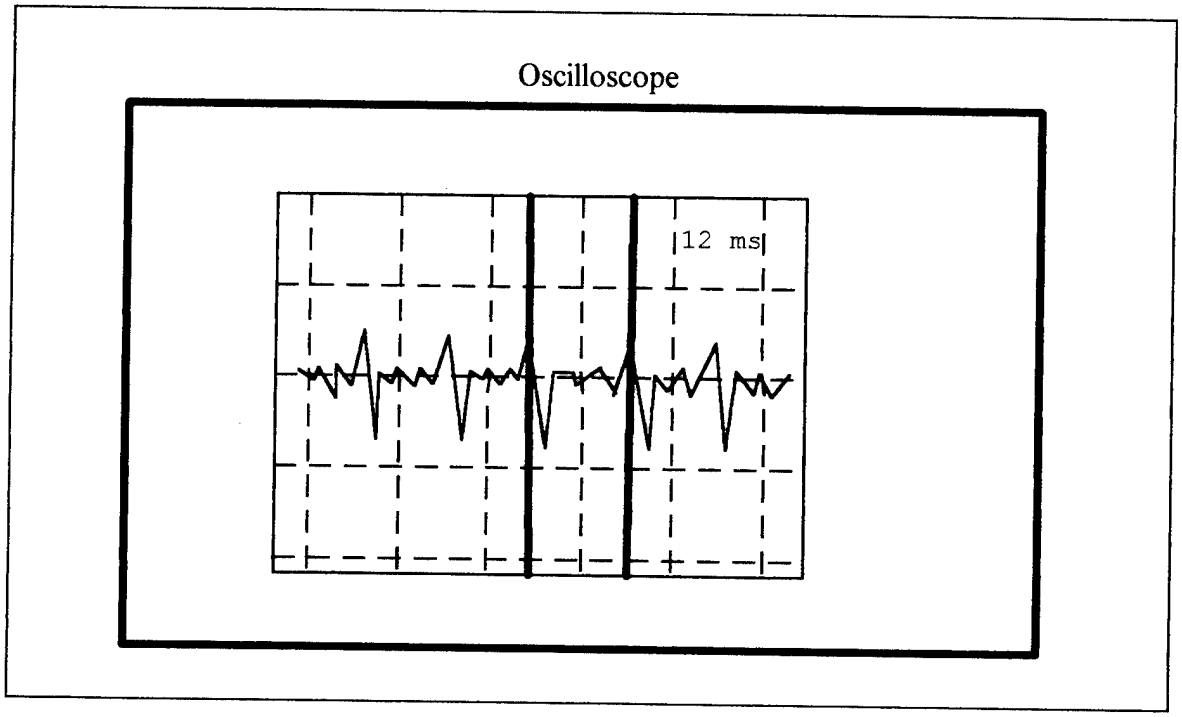

Figure 10 - O-Scope Measurements

a Philips PM 6669 Universal frequency counter. Both the frequency counter and o-scope were calibrated prior to the tests by exciting them with a known frequency from a Wavetek Model 142 HF VCG frequency generator, and reading the output. The third method used a Futaba Tacho-Sensor optical sensor which was attached to a support on

the ADF and aligned through the prop. Since the propeller had three blades, the frequency observed by the optical sensor was divided by three to give the actual rpm of the engine. The optical sensor was calibrated by observing a light source at a known frequency.

Prior to taking any rpm measurements, it was determined through previous thesis testing [Ref. 18] and from the AROD manual [Ref. 15] that an idle throttle was roughly 3000 rpm whereas a full throttle was 7800 rpm. Therefore, the engine was measured at idle, half throttle and full throttle with readings being taken off each sensor at those settings. Using the above rpm approximations, the idle, half, and full throttle were assumed to be 3000 rpm, 5400 rpm, and 7800 rpm respectively. That method, whose readings most closely resembled the above approximations, would be the method used for determining rpm calculations for the remainder of the tests. The results are shown in Table 2.

Run #1						
Throttle	Freq Counter	Calc. Rpm	Optical Sensor	Calc. Rpm	O-scope (ms)	Calc. Rpm
Full	138	8280	3400	1133	7.7	7792
1/2	86	5160	2800	933	8.88	6756
Idle	17	1020	2000	667	18.8	3191
Run #2						
Throttle	Freq Counter	Calc. Rpm	Optical Sensor	Calc. Rpm	O-scope (ms)	Calc. Rpm
Full	146	8760	3200	1067	7.5	7999
1/2	89	5340	2900	967	9.2	6521
Idle	34	2040	2000	667	18.24	3289

Table 2 - Rpm Calibration Results

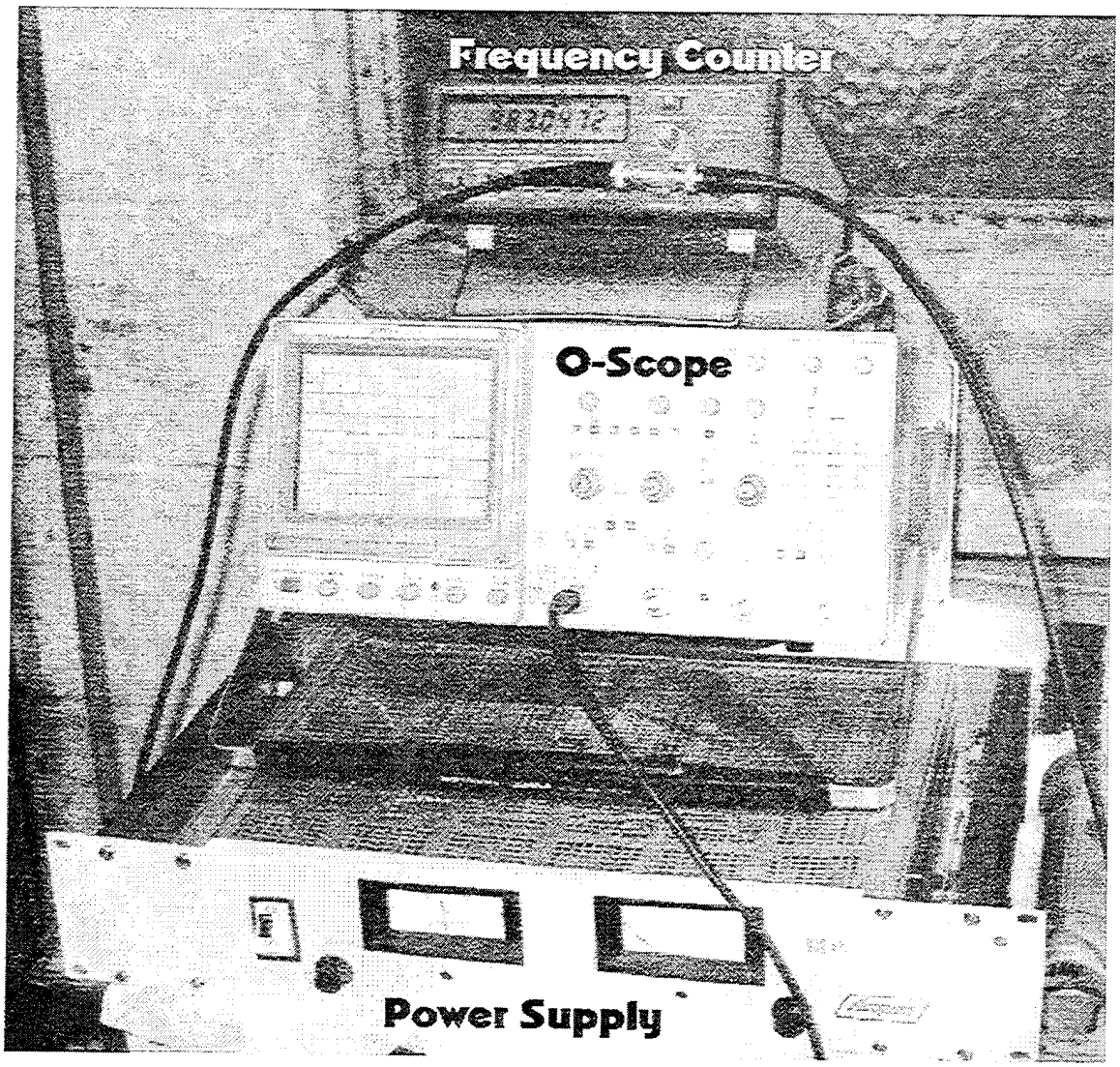

Figure 11 - RPM Calibration Setup

To read the rpm output of the tachometer, a line was first connected to the signal output on the ignition circuit. The frequency counter and o-scope were connected in series so the output signal was first fed into the frequency counter and then the o-scope (Figure 11). For the frequency counter, 1-second, 2-second and 10-second measurement times were all selected with the 10-second interval proving the most consistent. The

optical device was taped to a leg of the ADF and pointed through the prop arc of the vehicle.

It was obvious from the above results that the oscilloscope provided the best means for rpm determination. The easiest method to read was the frequency counter, but the amount of noise that was present in the signal was excessive and resulted in erroneous readings. The optical sensor was very inaccurate, probably due to the extensive vibrations of the ADF engine while running.

After a reliable method was obtained to ascertain engine rpm, thrust and fuel usage data were determined for the engine. Previous research had determined rpm vs. thrust and throttle position vs. thrust for a similar ADF engine [Ref. 18]. The objectives for continued thrust tests were to confirm whether this engine had the same characteristics as the previous engine tested, and if so, could that data be used in flight control calculations to be determined later. Additionally, fuel usage data allowed for estimates of flight times for the air vehicle at different rpm settings.

2. Thrust Stand Tests

Both the ADF engine and the one tested in Ref. 18 were rated for the same thrust output, as the engines were identical and both propellers were fixed at 14° tip blade angle. Therefore, the expected rpm and thrust outputs of the two engines should have been equivalent.

The ADF was mounted in the thrust test stand (TTS) as shown in Figures 12 and 13. No mufflers were used and the control vanes were removed prior to engine runup to

replicate the test conditions in Ref. 18. Also, this configuration eliminated blockage effects and ensured accurate thrust measurements. The TTS was designed to measure both thrust and torque, but since the tests were only concerned with thrust, the vehicle was secured in the stand to mitigate any rotation due to torque effects. To measure thrust, two spring loaded thrust gauges were used. The first was capable of measuring up to 100 lbs of thrust while the second measured up to 50 lbs. Therefore, the second gauge was set back slightly so that it engaged the thrust plate at about 70 lbs of thrust. The total thrust was then found by simply adding readout of the two gauges.

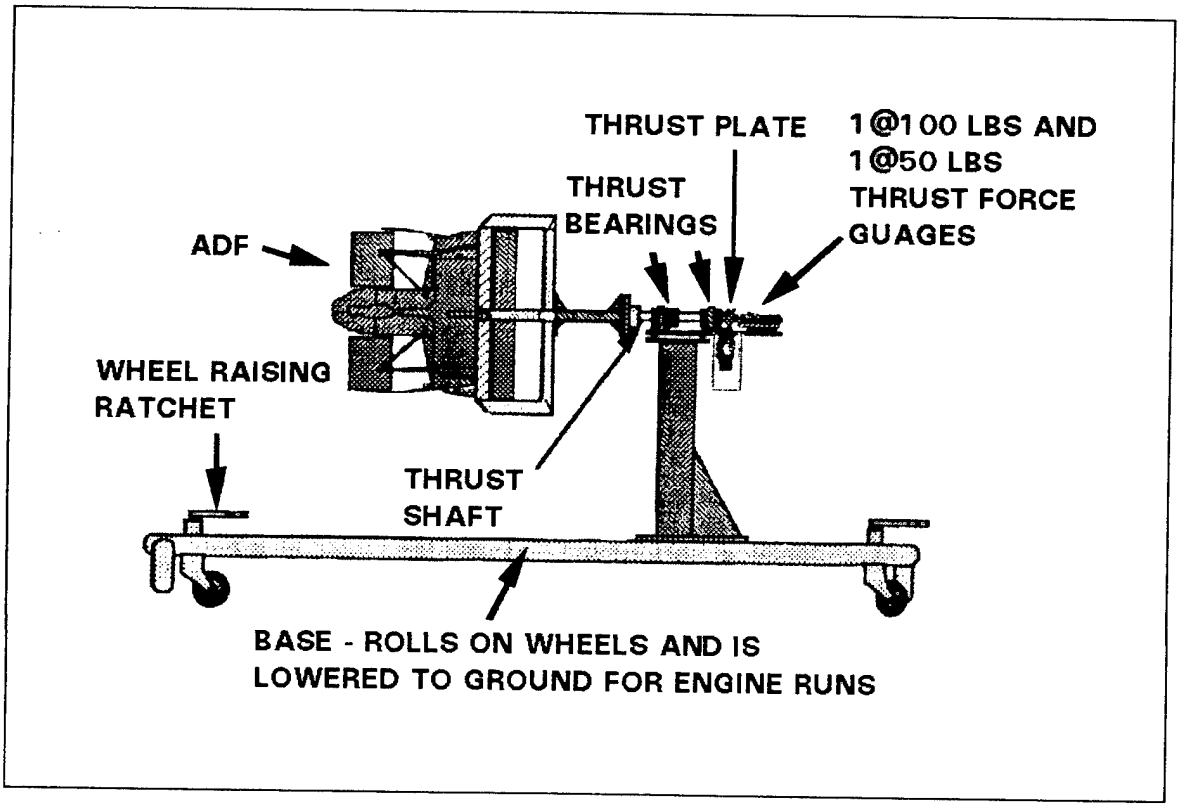

Figure 12 - Thrust Stand

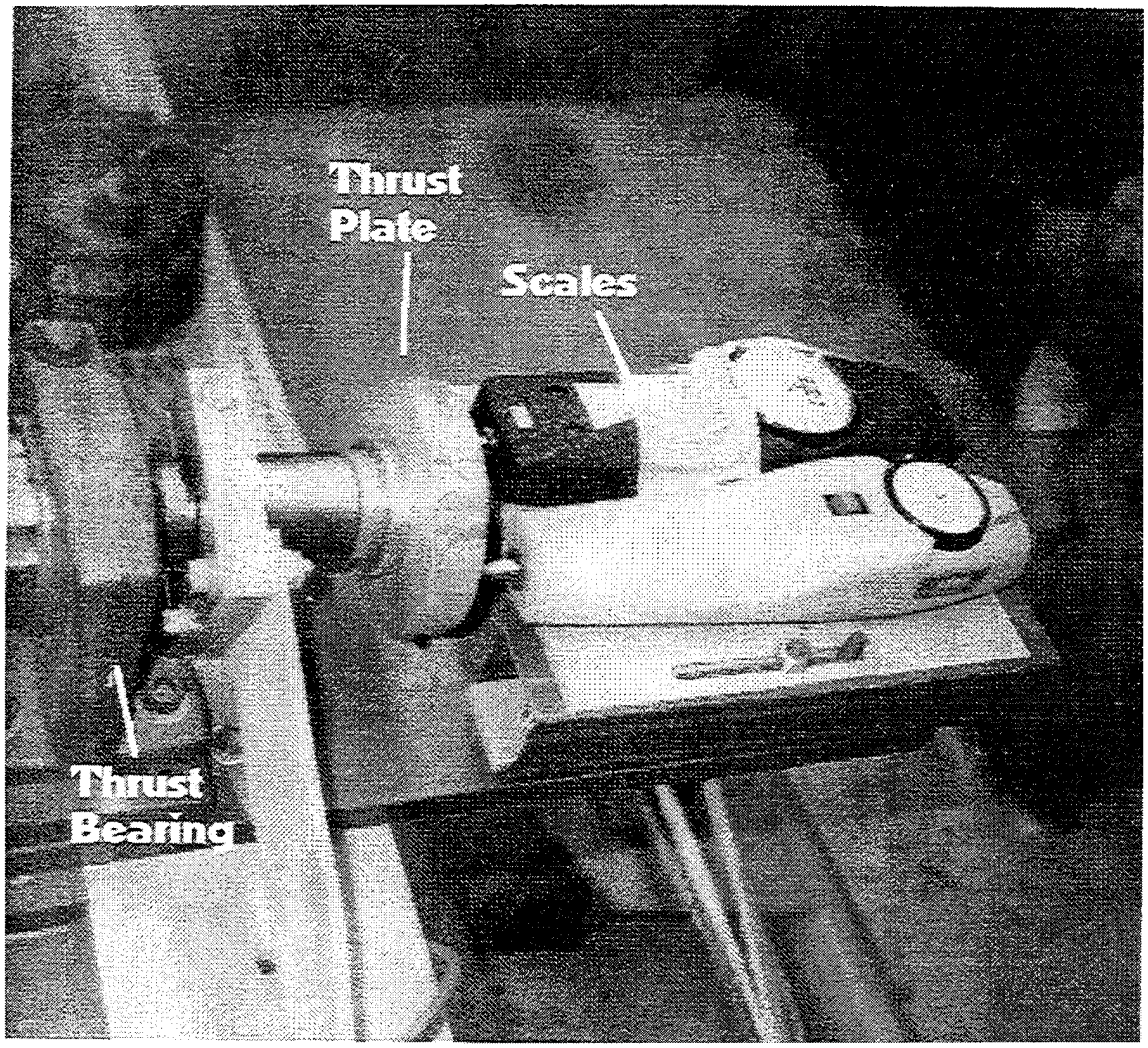

Figure 13 - Thrust Gauges

The objective of the tests were to replicate previous engine testing and correlate the results if possible. Tabular data are contained in Appendix C while the graphical data are shown in Figures 14 and 15. These figures show the relationship between the previous

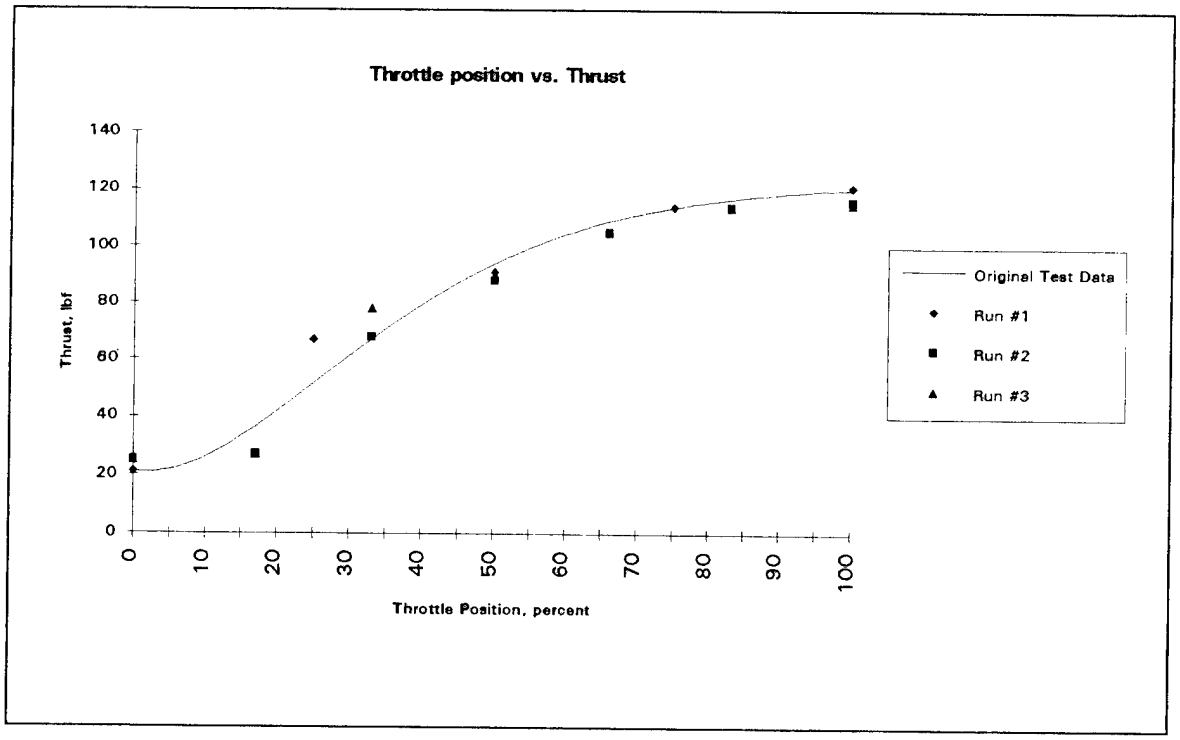

Figure 14 - ADF Engine Test Results / Thrust Vs. Throttle Position

data and the current data for the ADF engine. For Figure 14, the solid line represents a curve fit of the results in Ref. 18 while runs 1, 2 and 3 are the throttle position versus thrust data for the ADF. A curve fit for the ADF data was done and nearly overlaped the original data; therefore, it is not shown. Equations for curve fit data are found in Appendix E. This excellent correlation of previous data against current data was consistent with the fact that the two engines and propellers were similar.

The thrust versus rpm data in Figure 15 show an interesting difference, however, in the two data sets. A curve fit to the original data is again shown with a solid line and a curve fit for the ADF data is represented by the dashed line. Several data points were not used in the curve fit as they were inconsistent with the other results, but subsequent

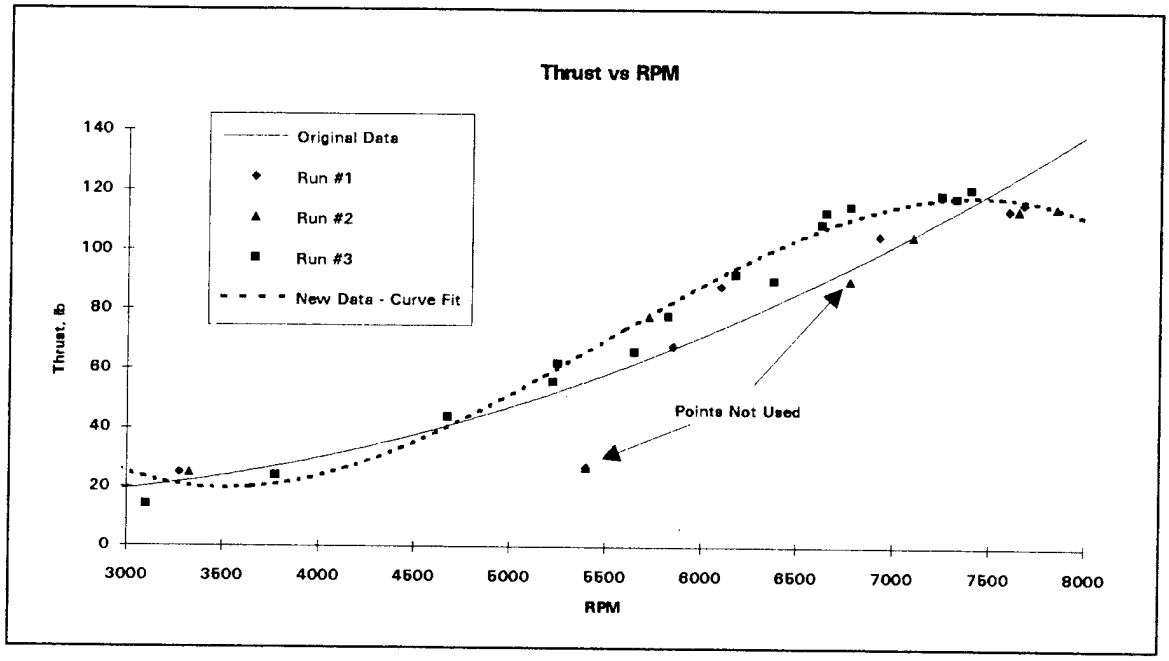

Figure 15 - ADF Engine Test Results / Thrust Vs. Rpm

similar data points did appear to provide good data. The original data set showed the thrust continuing to rise as engine rpm increased while the current data set suggested that not only did the thrust stop rising, but rather it decreased slightly near maximum rpm output. This decrease suggested that the maximum thrust output of the engine/propeller combination did not correlate with the maximum engine rpm. One possible reason for the discrepancy was that ADF thrust test data were concentrated toward higher rpm, where the vehicle would be operating in flight, whereas the data from Ref. 18 was spaced evenly over the thrust spectrum with only a few data points in the upper ranges. From the data in Appendix C, it can be seen that the maximum thrust occurred at 7400 rpm whereas the maximum rpm of the ADF engine was approximately 7650 rpm.

B. WIRING / VIBRATION

1. Problems

One particular problem that came to light during the initial engine testing phase was that of an internal wiring deficiency. This included the wiring that ran internally down the ADF which supplied power and control inputs to the vane and throttle servos, as well as the ignition wires. As the ADF was running, the engine produced a significant amount

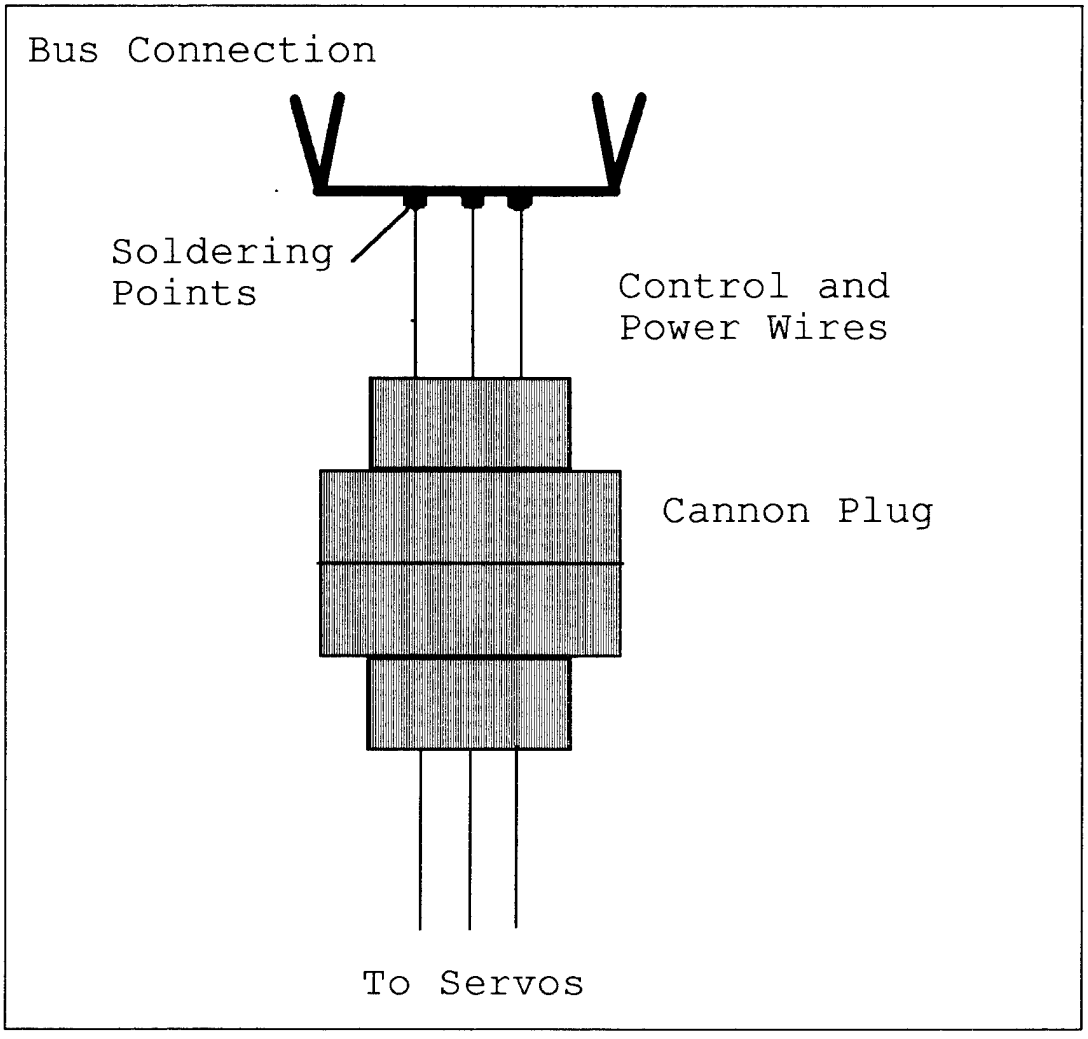

Figure 16 - Wiring Connections

of vibration which in turn rattled the wire connectors (cannon plugs) within the machine. As these plugs shook continuously during the course of the tests, they put stress on all the wires to which they were attached. Many times, these wires were merely soldered to other connections so these connections quickly broke away; thus all inputs were lost to the servos. In flight, the resulting failure could be catastrophic, considering all power and control inputs could be lost instantly. Additionally, ignition wires also failed, causing loss of a power source, whether it was generator or externally generated. This problem was never addressed by Sandia since the wiring was slightly different. There, the connectors (cannon plugs) were not incorporated so the additional stress on the wires was never realized. However, cannon plugs were incorporated in the design at NPS in order to decrease the difficulty in the troubleshooting process. Previously, repair work on the wires required removal of the engine which was time consuming, but by providing cannon plugs, access to wires was increased, thus decreasing repair times.

There were several possible solutions to these problems that needed to be addressed prior to any inflight testing of the vehicle. The first solution was to use a larger gauge wire when soldering connections, so that the wires would be able to better withstand the continuous engine vibrations. The second was to coat the connections in a type of silicon, similar to that used in the ignition circuits. This reinforced the connections but made maintenance slightly more difficult. A third solution was to provide foam padding internally to absorb the vibrations while restricting movement of the plugs. This would be done in addition to the other methods discussed. Finally, cannon plugs could have been hard mounted within the body of the ADF itself. This allowed minimal

movement of any parts and provided the greatest strength. However, it also took the most time to complete and was the least flexible as far as maintenance was concerned.

2. Solution

The first solution to correct the wiring deficiencies was to mount the cannon plug connectors to a flat plate that was attached to the underside of the ignition circuits

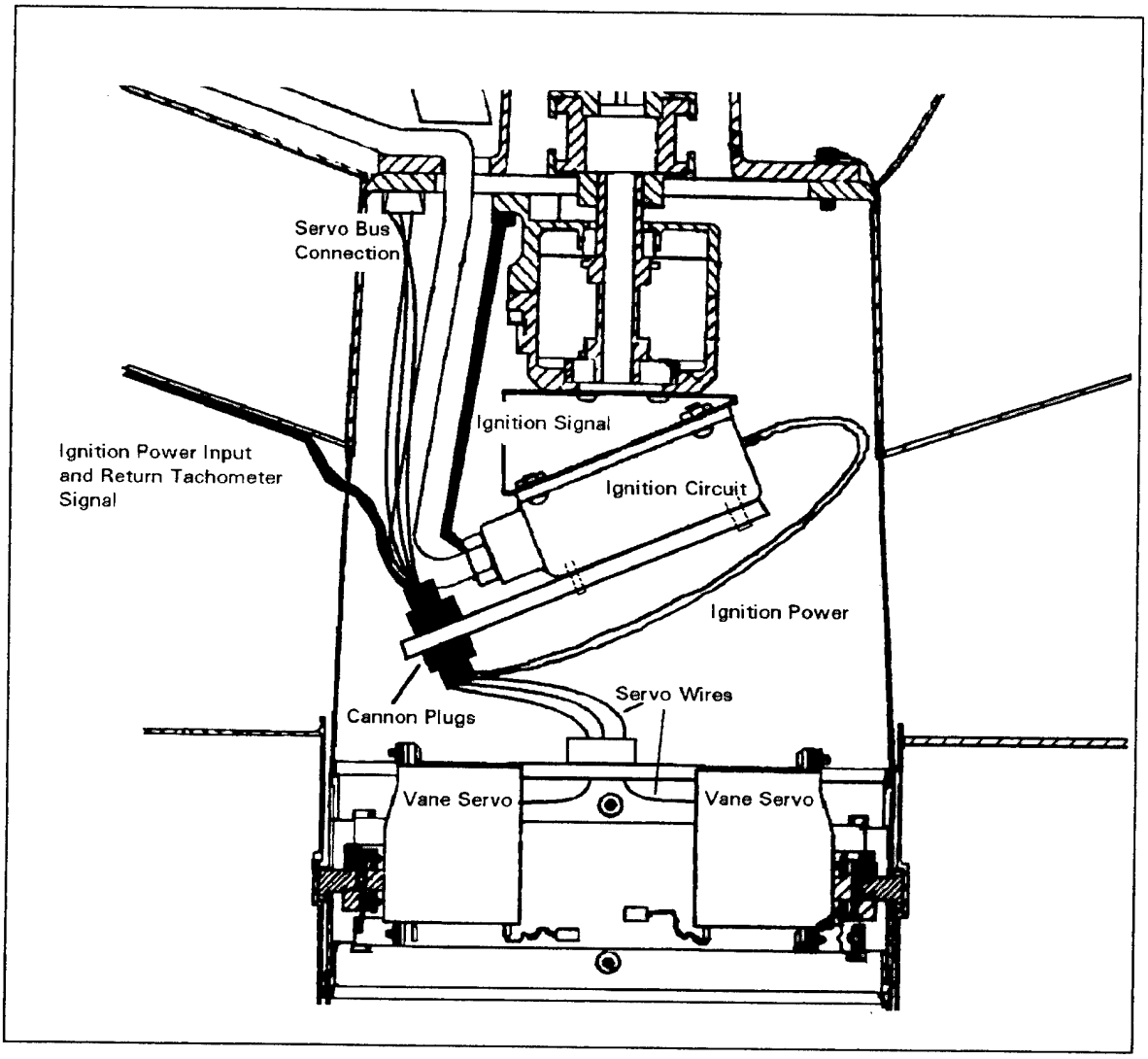

Figure 17 - ADF Wiring Corrections

(Figure 17). Both the plugs for the servo power and control and the ignition power were mounted using a small aluminum (4-1/4"x3"x1/8") plate that was tightened via screws used to hold the ignition circuit board in place.

Once the Cannon plugs were mounted firmly to the aluminum plate, the servo power was connected using 20 gauge wire instead of the 24 gauge wires used previously. The larger wires provided significant added strength in the soldered connections. Next, the 21 pin ITT connector used for the ignition power, was replaced with the cannon plug described above. The 24 gauge wires were also replaced with 20 gauge wires and the remaining signal wires that ran through the serial connector, were replaced with a 20 gauge substitute, and run through the ignition power cannon plug.

By replacing and upgrading the wiring, and by hardmounting the connectors, the overall strength of the wiring was increased significantly. Therefore, the reliability of the wiring was raised to the point where hover and flight testing could continue without the worry of a catastrophic wiring failure.

V. FUEL SYSTEM AND ENDURANCE TESTING

When the vehicles were received from Sandia Labs, a complex fuel control system was partially incorporated on the vehicles, which would allow fuel to be taken from any one of four onboard fuel tanks (to be described later). The fuel tanks drained into a common fuel control valve which allowed fuel, from only one selected tank, to be used. Sensing devices were originally planned to be incorporated by Sandia, which would detect an empty fuel tank by sensing air in the fuel lines. The control valve would then select another tank to feed fuel to the engine. Air sensing devices could also be used to provide information on fuel remaining. However, these sensing devices were never installed at Sandia Labs; thus the fuel control system never operated as designed.

To compensate for this incomplete fuel control system, a redesign of the fuel system was installed on the vehicle which simply allowed for a gravity feed system to provide fuel from all tanks simultaneously. This fuel system did raise concern, as no method was now available to determine when the vehicle was running low on fuel. Therefore, extensive fuel endurance testing was done to allow predictions of fuel usage to fly the ADF safely over a range of engine rpms. Mission profiles could then be used to figure out the fuel required to complete any flight. The following is a description of the fuel endurance testing procedures and results, as well as a description of the new fuel system used.

A. FUEL ENDURANCE TESTS

After thrust data were obtained from the ADF engine, tests were run to determine the endurance of the engine running at different rpm. Engine rpm varied from approximately 3000 rpm to 7800 rpm, but according to the thrust data, the engine did not provide enough thrust until about 4500 rpm (assuming a vehicle weight of 80 pounds) to keep the vehicle aloft. Therefore, tests were designed to run from 4500 rpm until full throttle in 1500 rpm increments which included 4500 rpm, 6000 rpm and full throttle (7500-8000 rpm). The 6000 rpm setting was run for five, ten and 15 minute periods to ensure accuracy, since this engine speed relates to a fully-loaded vehicle in hovering flight (100 lbs). Additional runs of ten minutes each at target engine speeds of 5000, 5500, 6500, and 7000 rpm were used to better estimate the fuel used during all operational engine speeds.

For each of these rpm settings, the engine was run on the thrust stand using an external fuel supply. Fuel was measured out in a 2000 milliliter Kimax TD beaker. The lb/gal of the fuel was determined by weighing the beaker empty and then with fuel. The difference was the fuel weight for 2000 ml of fuel. A conversion factor of 2000 ml = 0.5283 gal was used. Prior to engine start, the same procedure was used to determine fuel used per engine run using the external fuel container. The external fuel container was weighed empty and then filled with fuel. The can was then simply weighed again before and after the engine run periods to determine fuel usage. Values for these runs can be found in Appendix D.

The reasons for the endurance testing were to determine the maximum endurance rpm while hovering, and to determine if there was a linear relationship between rpm and fuel consumption. According to the AROD manual [Ref 15], the onboard fuel tanks held approximately three gallons of fuel while the ADF engine consumed about three gallons of fuel per hour. Therefore, the ADF was rated at one hour of endurance per fuel load. Furthermore, specific inquiries were made as to the capabilities and endurance of the vehicle [Ref 6]. By determining duration of the fuel supply, it was also hoped to predict the increase in endurance if additional fuel could be carried.

Table 3 shows the results of fuel testing.

Run #	Desired RPM	ms (o-scope)	Actual RPM	Time (min)	Tank Weight, lbs (Before)	Tank Weight, lbs (After)	Fuel Used (Gal)	Endurance (Gal/Hr)
1	6000	9.96	6024	15	10.28	7.78	0.3978	1.5913
2	6000	10.00	6000	10	7.78	5.77	0.3198	1.9192
3	6000	9.94	6036	5	5.77	4.81	0.1528	1.8332
4	5000	11.84	5067	10	8.66	7.95	0.1129	0.6779
5	5500	11.1	5405	10	7.95	7.25	0.1114	0.6683
6	6500	9.17	6543	10	7.25	5.91	0.2132	1.2794
7	7000	8.6	6976	10	5.91	2.66	0.5172	3.1031
8	7500	7.96	7547	10	8.72	5.12	0.5760	3.4560
9	7200	8.27	7255	10	9.27	5.93	0.5340	3.2080
10	6800	8.81	6810	10	9.26	6.00	0.5219	3.1300
11	6300	9.43	6362	10	7.21	5.73	0.2369	2.0310
12	5800	10.29	5830	10	8.48	7.21	0.2033	1.2200

Table 3 - Fuel Testing Results

Fuel usage was plotted against both engine rpm and thrust output with results plotted in Figures 18 and 19. An ADF vehicle carrying all necessary instrumentation with

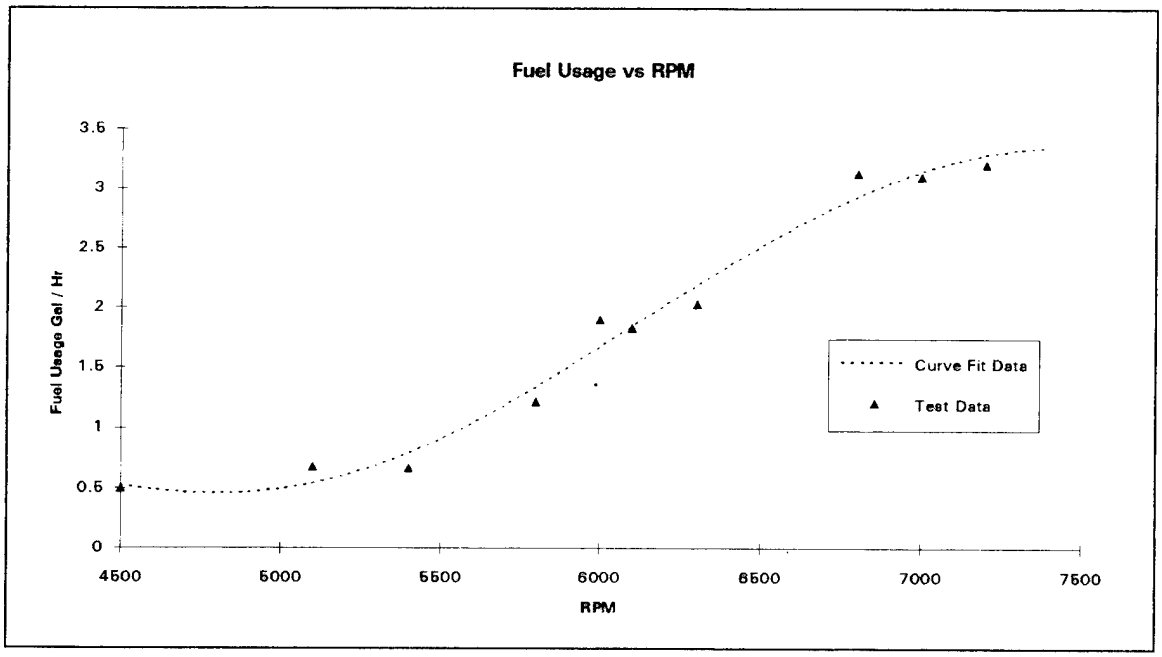

Figure 18 - Fuel Endurance Results

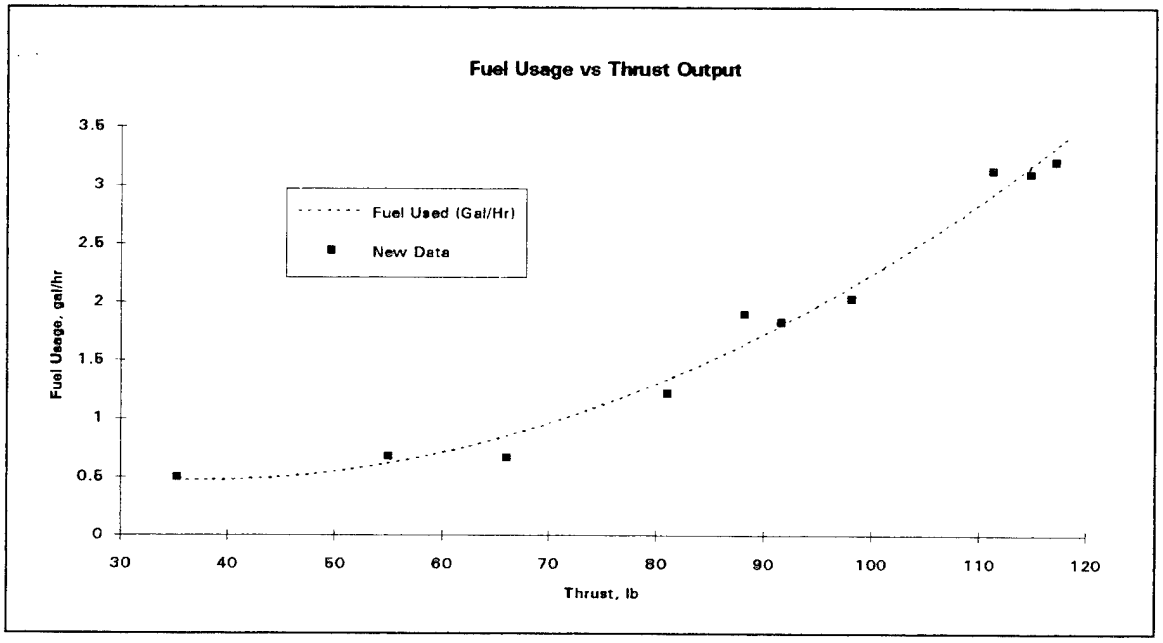

Figure 19 - Fuel Endurance Results

a full fuel load required about 90 - 100 pounds of thrust to hover which converted to an engine speed of 6000 rpm. At this ADF engine output, the vehicle consumed approximately 1.8 gallons/hour of fuel which extended the endurance of the ADF significantly to one hour and forty minutes, considering a 3.0-gallon fuel capacity. However, if the thrust output of the engine was set at full throttle, or 120 pounds, the fuel usage jumped to almost 3.5 gallons per hour which limits the endurance of the ADF to only 50 minutes. Therefore, any additional instrumentation added to the vehicle can substantially limit the endurance of the vehicle.

B. FUEL SYSTEM DESIGN

1. Fuel Tank

The fuel tank was integral to the shroud and consisted of four separate containers in the volume above the spar (Figure 20). The fuel was stored within these containers and had roughly a 3.0-gallon capacity that supported approximately one hour of operation [Ref 15]. Internal separators located at each quadrant divided the tank into four independent sections while baffles, located in each fuel tank, were used to reduce fuel sloshing and the resulting adverse dynamic effects on vehicle stability (Figure 21). The baffles were merely partitions molded within the fuel tanks with three small holes to allow limited fuel flow. Fuel was taken equally from each tank segment via a gravity feed system designed to minimize vehicle imbalance about its vertical axis. The fuel fed simultaneously from all four tanks into a small header tank located lower down on the spar.

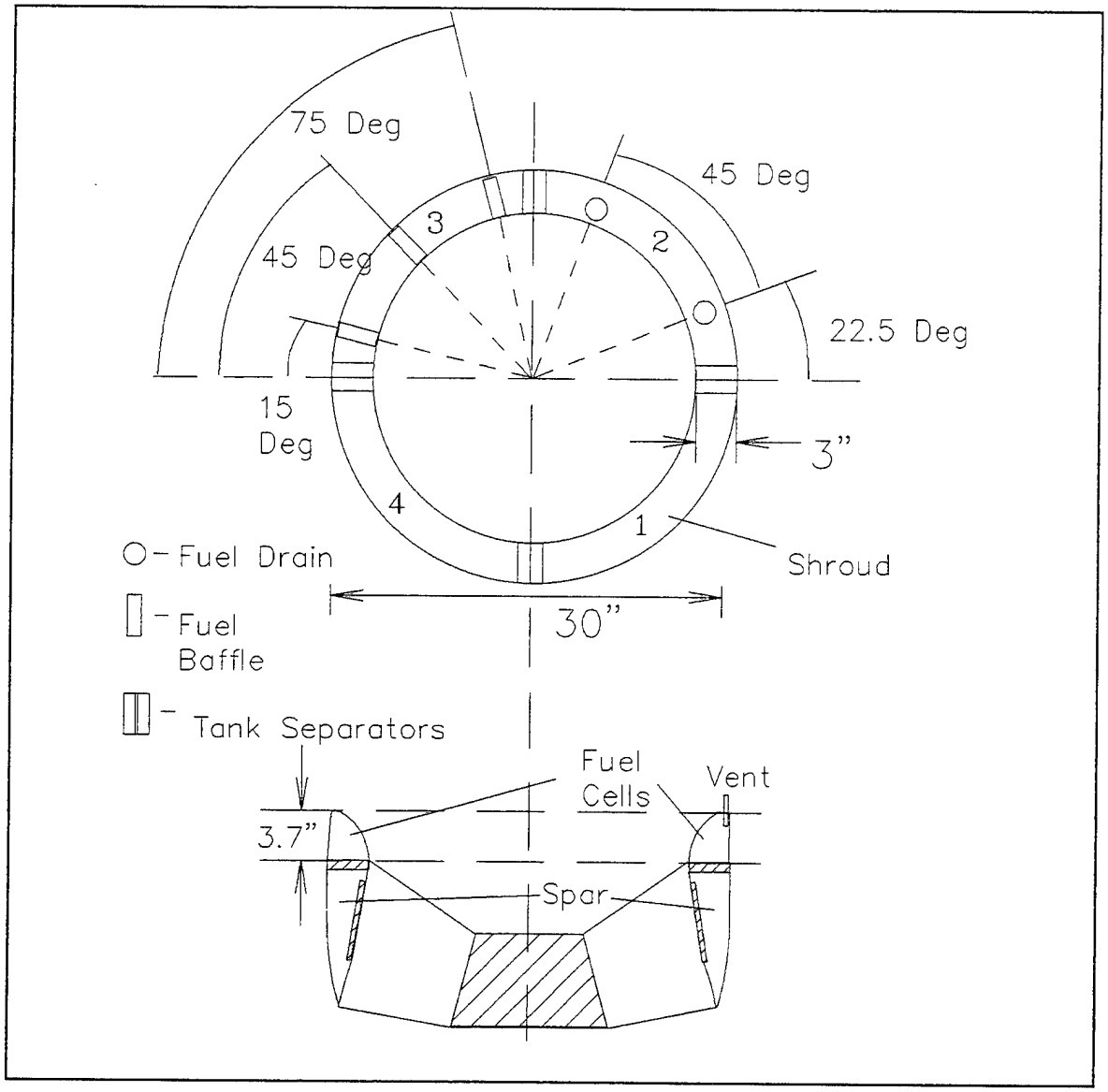

Figure 20 - Fuel Cell Diagram

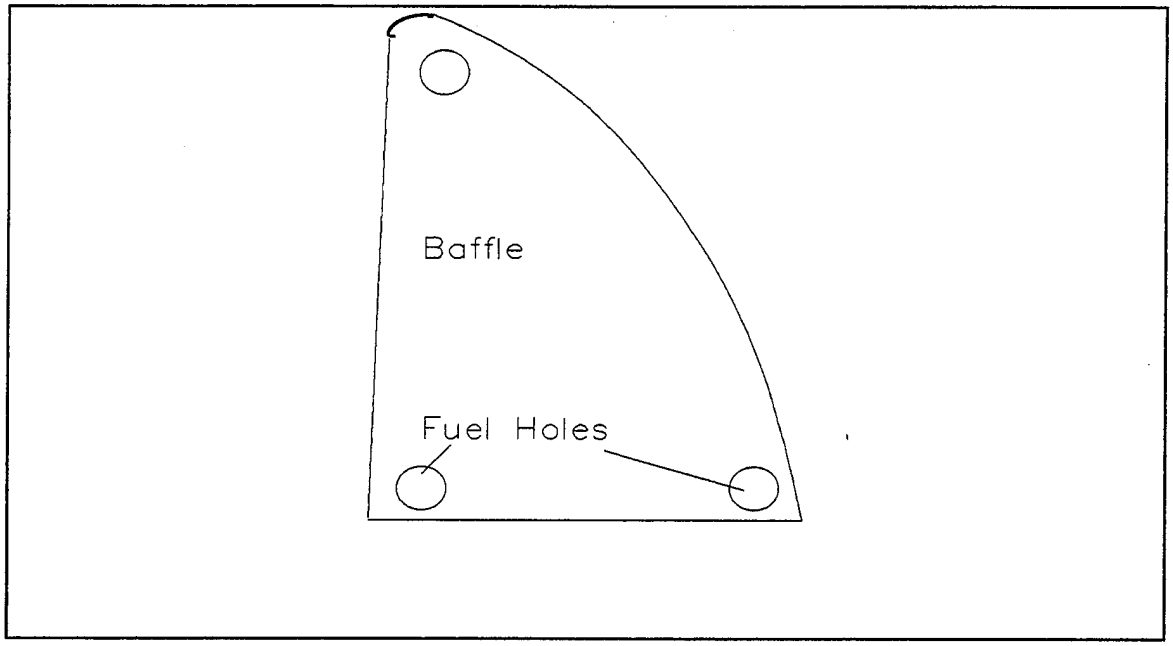

Figure 21 - Fuel Baffle

Fuel used was a combination gasoline / oil mixture (80:1), which was standard for a 2-stroke 2-cylinder engine such as the one used. The oil used for all engine operations was Opti-2 2-cycle engine lubricant. The vehicle was fueled through a pressure-feed system which allows all tanks to be filled simultaneously.

2. Fuel System

The fuel system consisted of the fuel tank (see Section V.B.1, above), a header collection tank, a primer pump, a fill valve, and vacuum-driven fuel pumps on each carburetor.

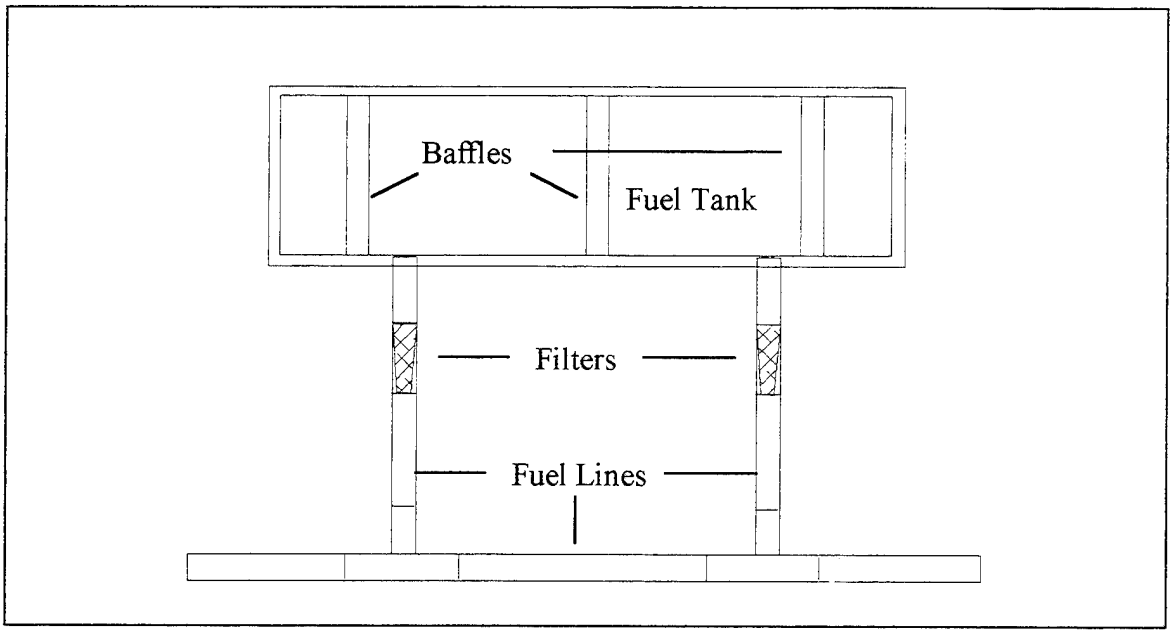

Figure 22- Fuel Tank Layout / Feed System

Each tank segment drained by two fuel lines located adjacent to the separating partitions, i.e., at the "corners" of the tank segment (Figure 22). Two lines were used to ensure that fuel flow from each segment regardless of fuel level and vehicle pitch (both forward and side). At any vehicle orientation, fuel should be present in one "corner" of each tank segment. The fuel flowed out of the fuel tanks through small filters to ensure there is no fuel contamination when the fuel enters the engine. All four fuel tanks were connected via a fuel line that runs horizontally around the vehicle approximately 6.5 inches below the fuel tanks. This fuel system design, in essence, connected all the tanks so they act as one large fuel tank. Each of the four tanks also had a ventilation tube so the fuel flows smoothly out of each tank towards the engine.

The fuel was collected in a four-ounce header tank which served as the sole source of fuel to the engine (Figure 23). Fuel was drawn equally from each tank by means of a

vacuum-driven fuel pump in each carburetor, through the header tank, and into the engine. The remaining fuel was evenly distributed in the peripheral fuel tanks and thus minimizes vehicle imbalance.

Neither fuel meters nor fuel tank gages were incorporated into the fuel system, but total fuel consumed can be estimated at any point in a mission by multiplying elapsed vehicle running or operating time by the engine fuel consumption rate during hover.

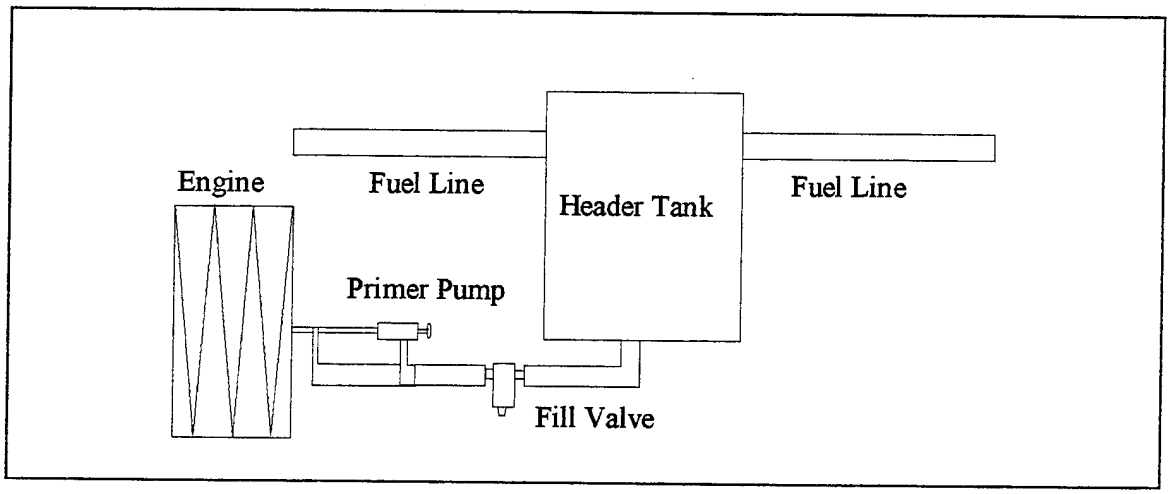

Figure 23 - Fuel Supply System

A primer pump was attached to the flow line just after the header tank and was connected directly to the two cylinders on the engine. To use the pump, it had to be turned and released from a stored position; otherwise the fuel was not allowed to flow through the primer, disabling its use. This prevented flooding of the engine when the primer was not in use. Once the primer was released, only several pumps were required and the pump was then restored to its locked position.

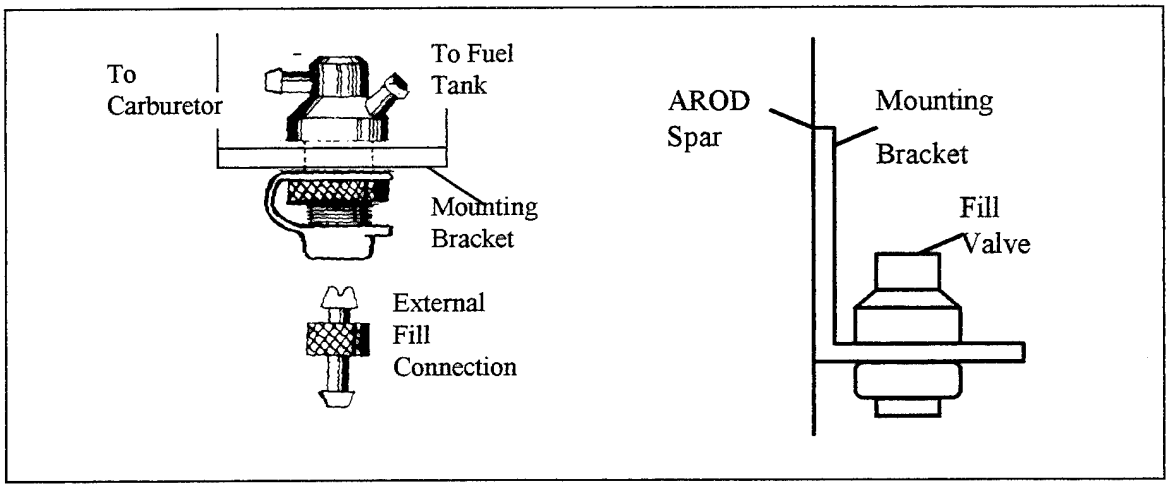

Figure 24- Filling Valve

To fill the fuel tanks, a fill valve was connected between the header tank and the primer pump (Figure 24). The fill valve was mounted on an "L" bracket and held rigidly in place for easy filling. When the external fill connection was not connected to the fill valve, the connection between the header tank and the engine was opened, allowing fuel to flow as required to maintain engine operation. When the external fill connection was in place, fuel was supplied from an outside source via a pressure driven pump. In this connected position, the fuel was prohibited from flowing into the engine but rather only into the header tank, and thus the four fuel containers located in the shroud. Since no fuel gauges were incorporated, fueling was completed when the four ventilation tubes overflowed.

Prior to using the fuel tanks in the ADF itself, another AROD airframe, used for parts, was cut open so the fuel tanks inside could be examined. A viscous residue, which appeared to be from the epoxy used in the fabrication of the fuel tanks, was found coating the bottom of the fuel tanks. It was uncertain whether the residue was harmless or rather the result of an unknown reaction between the fuel and the epoxy. To find out, a portion

of the fiberglass fuel tank was cut away and immersed in fuel for approximately two months. After this time, there was no noticeable deterioration of the fiberglass, so it was assumed the residue was harmless.

C. ENGINE TEMPERATURE DETERMINATIONS

During the fuel endurance testing, temperature readings were also taken of both the exhaust gases and the cylinder head by using thermocouples that attached to one of the exhaust ports and to a spark plug. The objective was to determine whether the engine could withstand excessive operating times and rpms without overheating. Both the exhaust and cylinder head temperatures were monitored over a large range of engine speeds and plotted in Figure 25. Run times varied from between five and 15 minutes in length. Engine speed was varied over a range from idle to full throttle but was weighted toward operating values in the upper range.

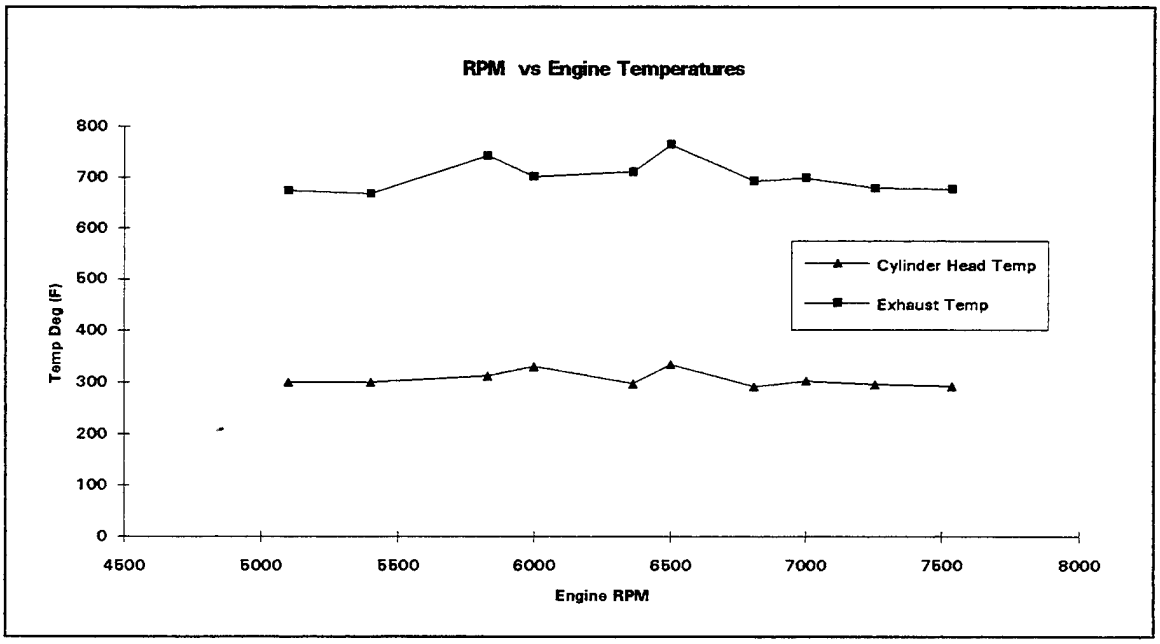

Figure 25 - Temperature Distribution

The spark plug was fitted with a 712-4wk Type J 0-700 F 1293 thermocouple with a 26 mm gasket attached. This sensing device was fitted in place of a washer that sat between the spark plug and the engine cylinder. This device was attached to measure the cylinder head temperature throughout the tests. To measure exhaust gas temperatures, a hole was drilled in one of the exhaust ports and a 712-4dwk Type K 0-1900 F 894 thermocouple was inserted and secured (Figure 26). The resulting temperatures were read on an Analog Devices 12 channel AD 2051 digital thermometer.

Total engine run time for this portion of the testing was about four hours, and from Figure 25, it appeared the temperatures remained steady throughout the tests, with several spikes occurring at 5830 rpm and 6500. These spikes appeared when the engine was warm and primed with fuel, probably due to irregularities in fuel flow. As more fuel accumulated in both the cylinder head and exhaust ports, the engine burned hotter initially, but temperatures dropped slightly as fuel flow evened out. Several five-minute run times were done, but the temperatures never evened out and the data were rejected. Short run times did not always allow the temperature in the engine to level out due to the effects described above.

Overall, it was apparent that the engine was consistent in its recorded temperatures in both the cylinder head and exhaust readings. From this, it can be reasonably assumed that run times of several hours should not significantly affect the engine performance in any way.

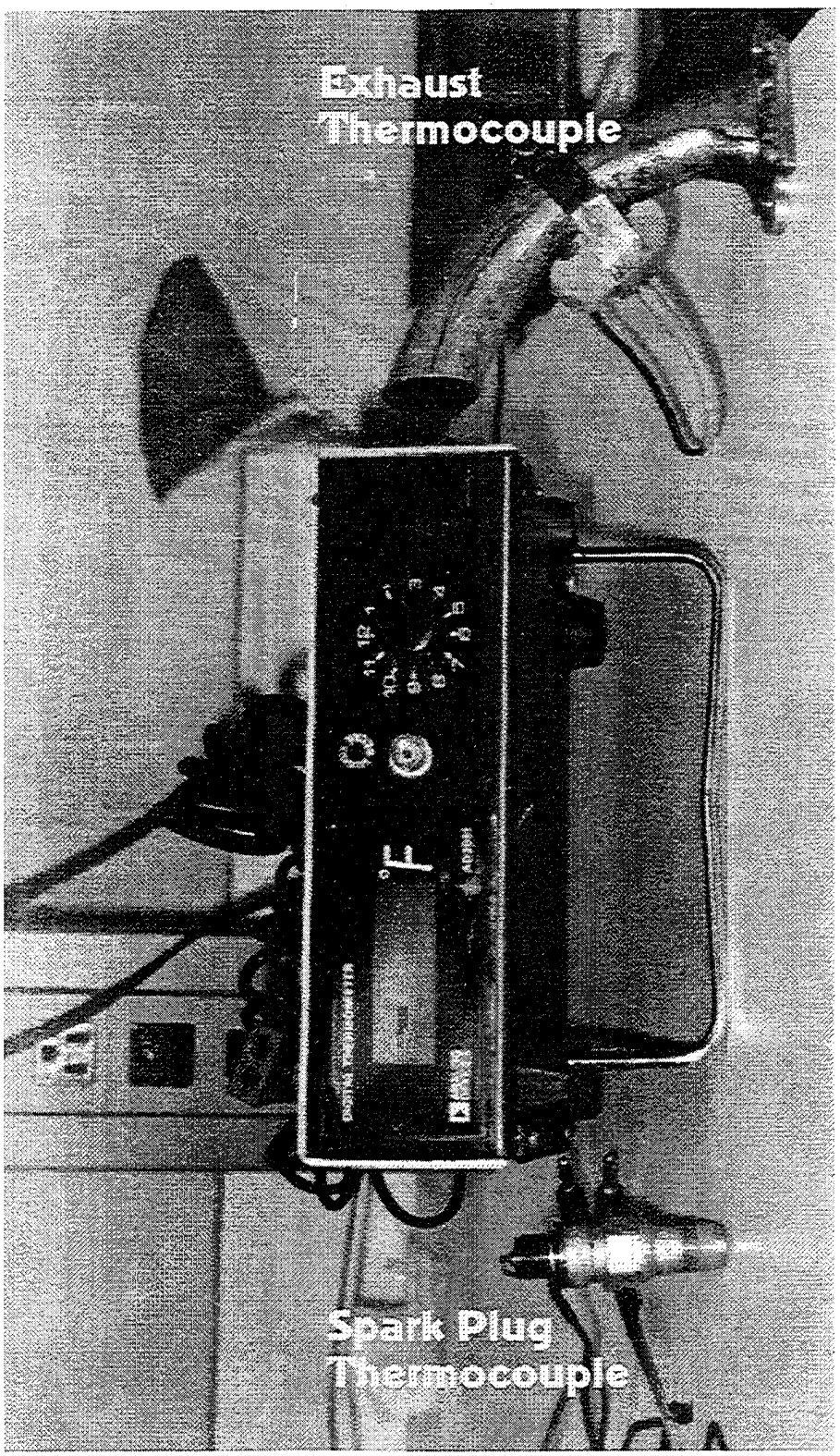

Figure 26- Temperature Thermocouples

VI. HOVER STAND DEVELOPMENT AND TESTING

A. HOVER TEST STAND DEVELOPMENT

The Hover Test Stand (HTS) was designed to allow the ADF to hover and rotate in a limited environment using an RF uplink for throttle and control vane instructions with feedback being received through an umbilical cord. The concept of incremental buildup [Ref. 19] was the guide for designing the HTS. Since the ADF had never flown at NPS, flight tests will begin with the ADF held motionless while throttle settings and control surface deflections are checked. The ADF would incrementally be allowed more freedom within the HTS confines. By using this method of flight testing, any problems, such as the wiring difficulties noted earlier, can be detected and corrected before further flights are conducted. Thus, flight testing would be safer with potential damage to the ADF being minimized.

The HTS was constructed out of angled 2"x2"x3/16" alloy 6061-T6 aluminum and the properties were found in Ref. 20 and listed in Table 4. This material was selected based upon strength, cost, and ease of use. The HTS was a large cubical frame, constructed from twelve eight-foot aluminum members (Figure 27). The HTS was bolted to a concrete surface so the frame remained rigid while the ADF was suspended within the frame.

The ADF will be suspended by adjustable ropes and have limited movement with six degrees of freedom. The maximum movement allowed will be three feet in three

directions with approximately 180° of pitch, roll, and yaw which would allow full testing of the flight control system prior to any free flight tests.

1. Strength Calculations

The 6160 T-6 angled aluminum was selected for its strength and ability to withstand any load the ADF could place upon it. The vehicle weighed approximately 90-100 lbs fully loaded with fuel and equipment and the maximum thrust output was about 120 lbs. These loads were distributed among the four vertical members in the HTS. For a factor of safety, it was assumed that each member would be required to support the entire load during any portion of the flight tests. The values in Table 4 made it obvious that the members can withstand the compressive effects encountered, however, a determination of buckling strength was conducted because of the length of the vertical sections.

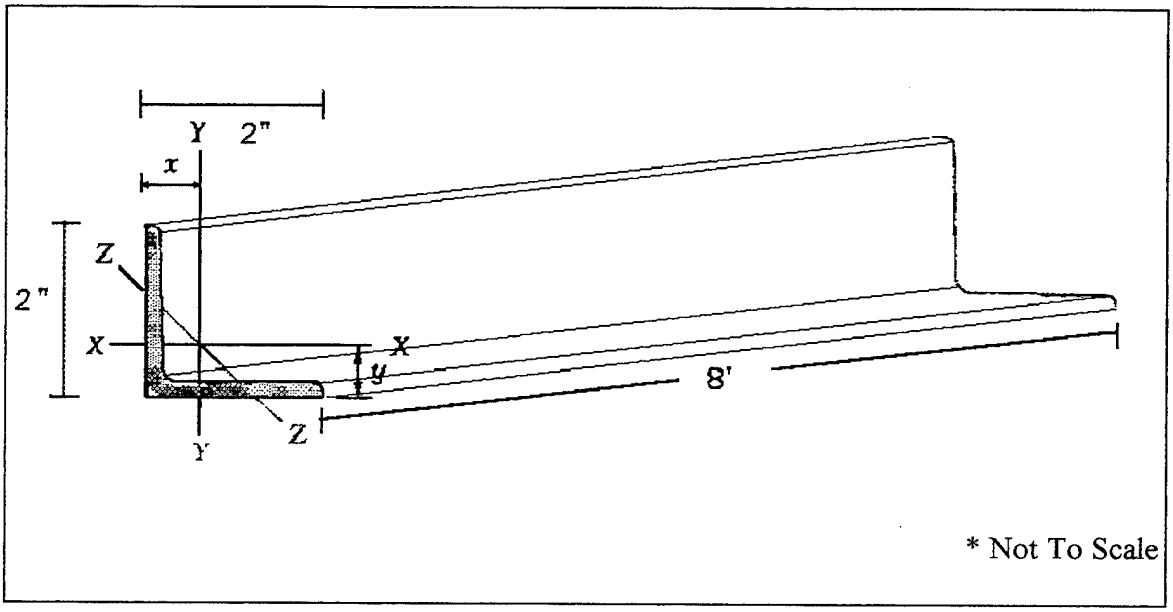

Figure 27 - HTS Cross-Sectional Area

To determine the maximum load (P_{CR} – Critical Buckling Load), the formula

$$P_{CR} = \frac{k\pi EI_{MIN}}{L^2}$$

was used with k being a constant, and the other variables being listed below. To increase the value of P_{CR}, only k could be adjusted since the other variables were fixed by material properties. Since k was a function of the types of end supports used [Ref. 21], adjusting k was done by increasing the support strength at the ends of the vertical members. This was done by adding guidewires and welding the corners of the HTS (see section VI.A.2, below) thereby creating rigid ends of the vertical members. The ends of the vertical supports then nearly resembled a fixed support, so k, and the critical buckling load, was safely increased.

Size and Thickness, in.	Weight Per Foot, lb/ft	Area, in^2	I, in^4	S, in^3	r, in.	x or y, in.	Axis Z-Z r, in.
L 2x2x3/16	2.42	0.711	0.269	0.189	0.6175	.569	0.3945
Material	Density, lb/in^3	Ultimate Tensile Strength, ksi	Yield Strength, ksi	Young's Modulus, 10^6 psi	Poisson's Ratio	Coeff. of Thermal Expansion, (10^{-6} / ^{0}F)	Ductility % Elong in 2 in.
6061-T6	0.098	42	36	9.9	0.33	13.0 (68-212F)	17

Table 4 - Section Properties

2. HTS Construction

The HTS was constructed as a large cube measuring eight feet on all sides. Restraining ropes made of nylon were attached from all sides of the ADF to all eight

corners of the cube. The ropes were adjustable so the ADF could be allowed controlled movement with six degrees of freedom. With the base of the HTS being an eight-foot square, the ADF was placed in the center on a raised platform (Figures 28 and 29). The platform was constructed of 20 gauge compressed metal and was attached to a moveable cart. The platform was 18 inches off of the ground and designed to limit the influence of ground effect as the ADF was lifting off. The grated surface of the platform provided

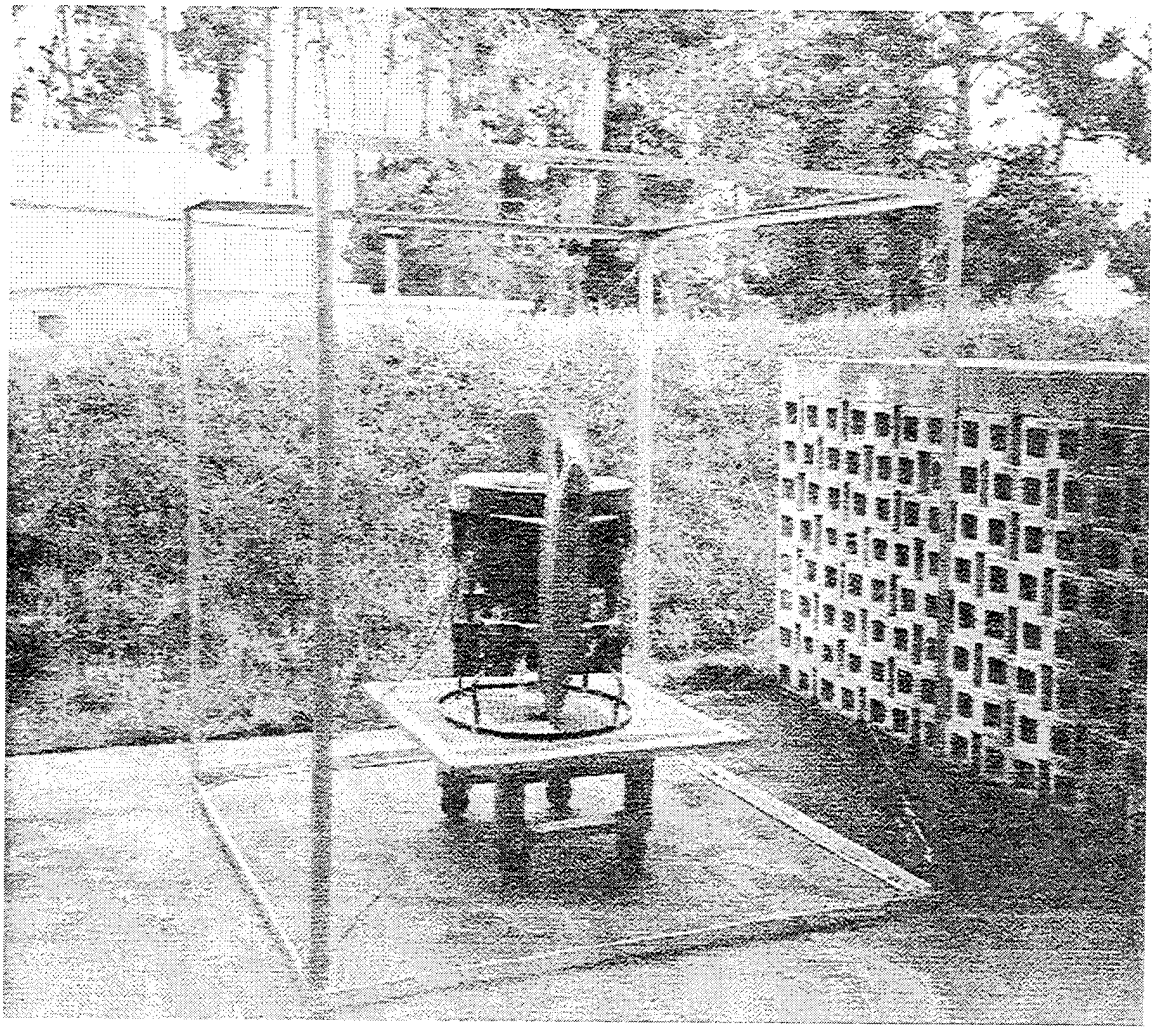

Figure 28 - HTS Construction

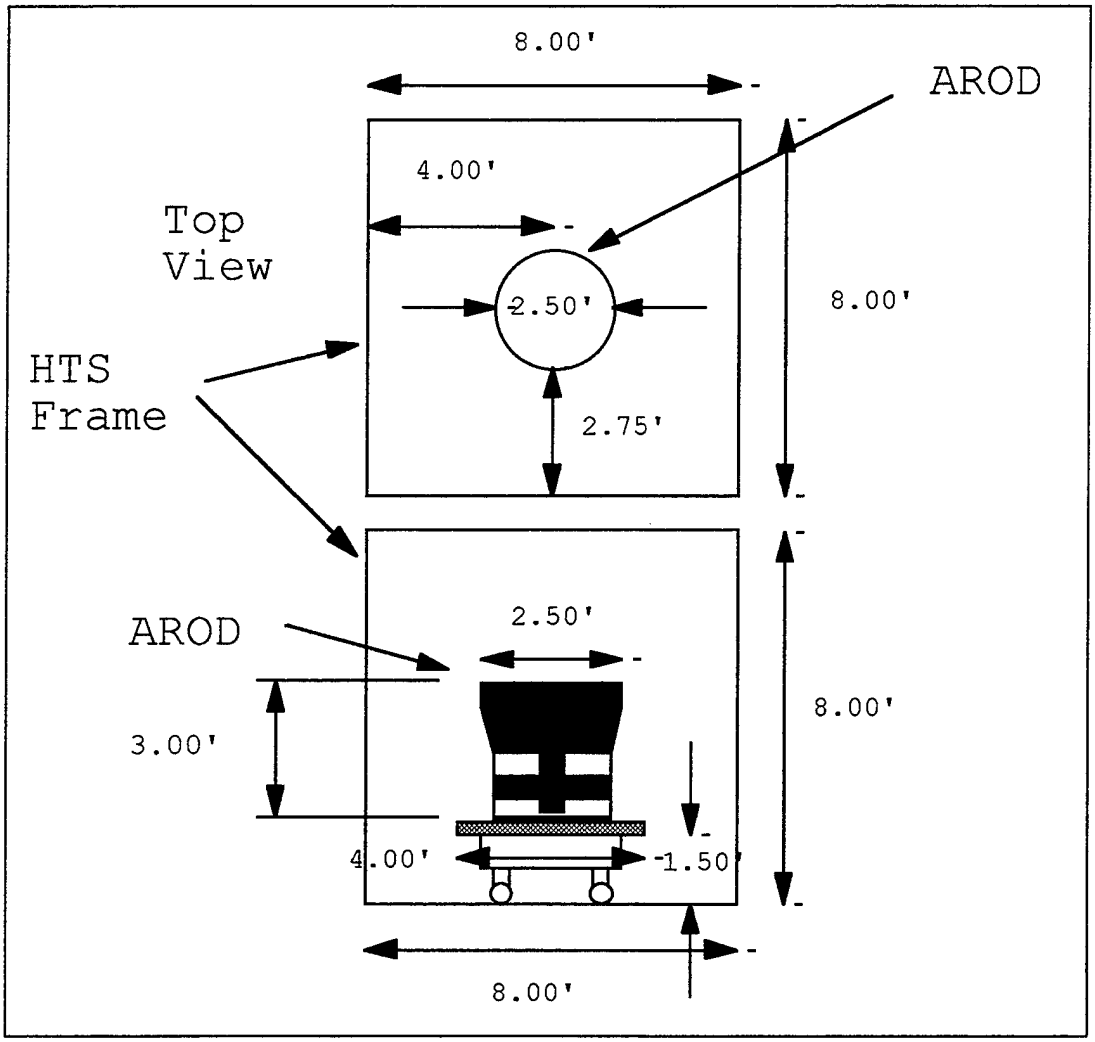

Figure 29 - ADF / HTS Positioning

little resistance while the vehicle was lifting off, thus minimizing ground effect. Since the cart was on wheels, it could be rolled out from underneath the ADF once it was airborne and replaced prior to landing.

The aluminum sections were bought pre-cut from a local machining shop. Both the top and the bottom members arrived with a 45-degree cut in the corners to enable them to fit together into a square shape (Figure 30). The members were welded together

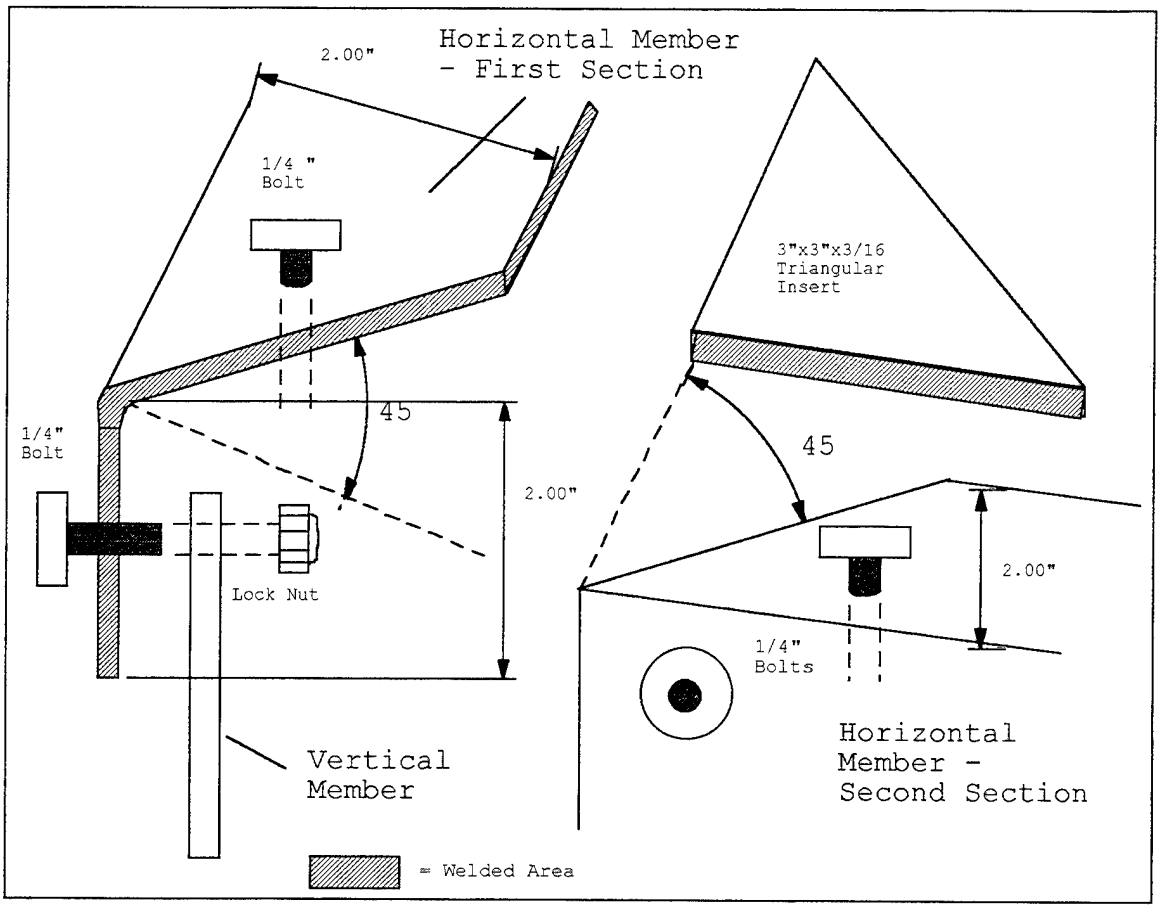

Figure 30 - HTS Connections

to increase the strength of the HTS prior to assembly. Next, a flat triangular 3"x3"x3/16" plate was cut and welded into the corners to increase torsional strength and provide an accessible surface from which to connect the restraining ropes.

After the top and bottom squares were welded together, the vertical members were modified to enable connection to the square pieces. To accomplish this, a small triangular (2"x2"x3/16") plate was welded to the inside of the section on both ends. Holes were drilled through the end plates and the sides of the vertical sections one inch from the ends. Bolts (1/4"x1") were used to make the remainder of the connections. When this was

finished, the cube portion of the HTS was complete. At this point, the cube was strong enough to support any static loads encountered, but torsional effects from the dynamics of the ADF could have exceeded the HTS's strength. To compensate for this, guidewires were attached diagonally in a large "X" on the sides to eliminate the torsional effects discussed above (Figure 28).

The guidewires were constructed of 1/8" steel wire and connected using S-hooks by drilling additional holes six inches from both the top and bottom of the cube. To tension the wires firmly, turnbuckles were used that allowed the wires to be pulled into place and strengthen the HTS. At this point, the only remaining task was to connect 1/4" eye-bolts through the 3"x3"x3/16" welded plates by drilling holes and using locknuts to tighten them down. Using these eye-bolts, it was possible to connect the restraining ropes to the ADF.

After the attachments were completed, the vehicle had 2.75 feet of movement in the horizontal direction, and 3.5 feet of freedom in the vertical direction. This was the maximum movement that was allowed. By adjusting the length of the restraining ropes through the eye-bolts, the vehicle can be held to the minimum desired movement.

3. ADF / HTS Connections

The ADF was secured inside the HTS by means of nylon ropes attached at each end to the ADF and the HTS. As mentioned earlier, the ropes were attached to the HTS simply by tying the ropes to the eye bolts located in the corner of the HTS. To fasten the ropes to the ADF, special aluminum fittings were made that allowed a secure connection.

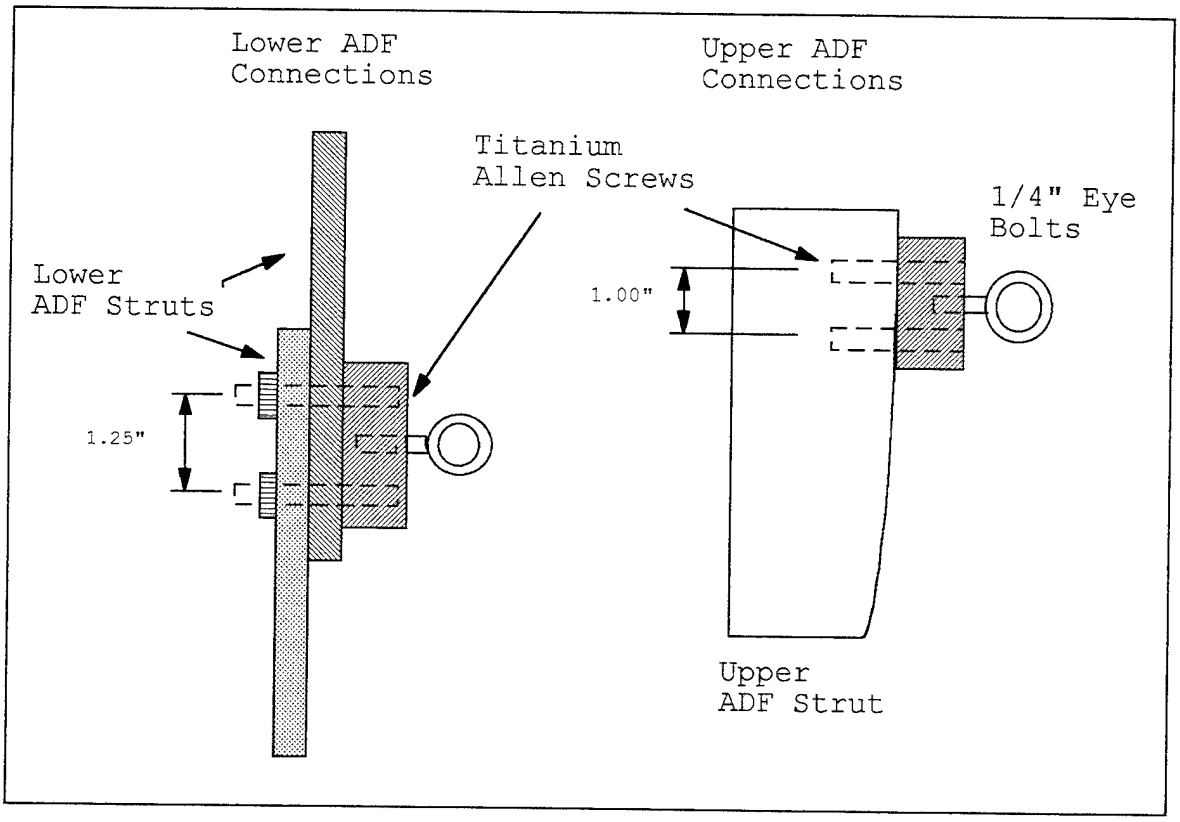

Figure 31 - ADF / HTS Connections

Figure 31 shows small aluminum blocks attached to the ADF by using 10x32x1" titanium allen screws. Eye bolts were counter-sunk into the aluminum blocks to use as connectors for the ropes. This end of the rope was looped around and spliced to itself to form a noose which attached to the eye bolt via a universal link. Had the link not been used, the eye bolt may have unscrewed from its mount as the ADF moved about the HTS. To avoid the rope from being ingested into the inlet of the ADF, several layers of shrink wrap were used to stiffen the rope so it could not bend around and become entangled in the inlet.

VII. CONCLUSIONS AND RECOMMENDATIONS

The objective of this thesis was to continue the development of a Vertical Takeoff and Landing Unmanned Air Vehicle that would be capable of real-time aerial reconnaissance while in hover or slow forward flight. To accomplish this, a UAV from a canceled Marine Corps program was modified by incorporating an advanced flight control system that would provide the VTOL UAV with the ability for autonomous flight. The Archytas Ducted Fan's development responded to a need for a UAV to provide real-time data for a number of missions including environmental study and coastal survey [Ref. 6].

The work on this project was two-fold. Firstly, another thesis student, working concurrently, designed a SAS that would allow for remotely controlled flight via an RF only link [Ref. 5]. Secondly, this current thesis tested and evaluated the characteristics of the ADF and incorporated the SAS on the vehicle in preparation for hovering flight. Initially, hovering flight will take place in a test stand where potential problems can be identified and solved. Finally the vehicle will fly untethered using only an RF uplink and downlink as its only communication with ground support.

At the time of this writing, the SAS has been operated successfully in the Avionics Laboratory using a simulator. Additionally, the rewiring of the ADF has also been completed and the SAS is now being installed on the aircraft. The HTS is constructed and awaits use as a testing platform for ADF hovering flight, and after the ADF is flown in the HTS, it will transition from tethered, controlled flight, to RF, untethered flight.

There is one point of concern when running the SAS in the ADF. Vibration proved to be source of difficulty with respect to the wiring and could be a problem for the avionics installed on the forebody of the vehicle. The IMU, which is the primary component in the SAS, is rated at 3 g's of acceleration in the x, y and z directions. This rating was provided by the manufacturer and should be sufficient to withstand any vibration on the vehicle. However, other components in the forebody are not rated in the same manner. The original Archytas Tailsitter encountered similar problems in its design, where electronics failed due to vibration, resulting in the electronics package being moved to the forebody [Ref. 16]. Extensive vibration testing with the present ADF configuration has not been completed although it is necessary to fully evaluate vibrational effects on the electronics.

One way to identify potential vibration problems, is to attach accelerometers to both the shroud and the forebody during initial HTS fight tests to determine the extent of the vibration over the entire vehicle. By locating the avionics in the forebody, it is hoped the supports for the forebody will dampen the vibration extensively alleviating the need for modification of the electronics mounts.

Another source of problems in previous Archytas testing was the noise present in the umbilical connector [Ref. 16]. Suggestions were made to shield the umbilical cable in order to reduce the noise, but such a solution is not feasible for the ADF in the long term. The umbilical cord is only a temporary connector until the RF downlink can be established, so further work on the ADF should concentrate on completing the RF downlink. All the required hardware and software has been purchased or developed and is

ready for implementation. Installation of a complete RF downlink will be a lengthy process, but nonetheless, it should be incorporated as soon as practical after initial flight tests.

Transitioning from the umbilical cable to purely an RF link abates the noise problem but presents an RF interference problem. During performance testing when using RF throttle commands, problems were observed with RF interference. During engine runups, individuals periodically walked between the transmitter and the receiver on the vehicle causing significant RF interference. The transmitter used at the time was a standard Futaba transmitter with an output of three-fourths of a Watt. When the ADF receives signals via the 486 PC, the signal should be strong enough to overcome this type of interference. The NPS FRL has applied for a military frequency that will be used only for its purposes which will allow for a strong signal without worry of local radio interference.

APPENDIX A: ADF DIAGRAMS

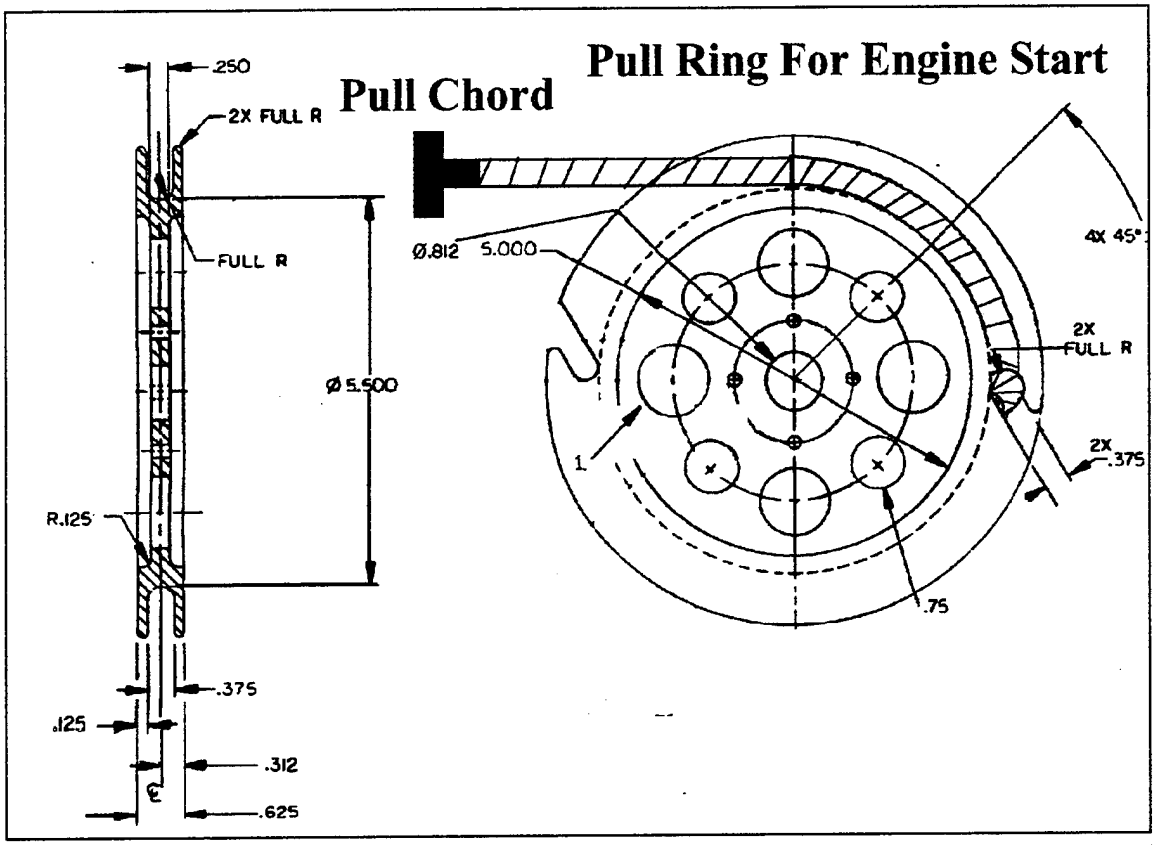

Figure A.1 - Pull Start Mechanism For The ADF [Ref. 15]

The Pull Start Ring is mounted on top of the main drive shaft. The vehicle is started much like a lawnmower in that the pull rope is wound around the ring and pulled to start the engine.

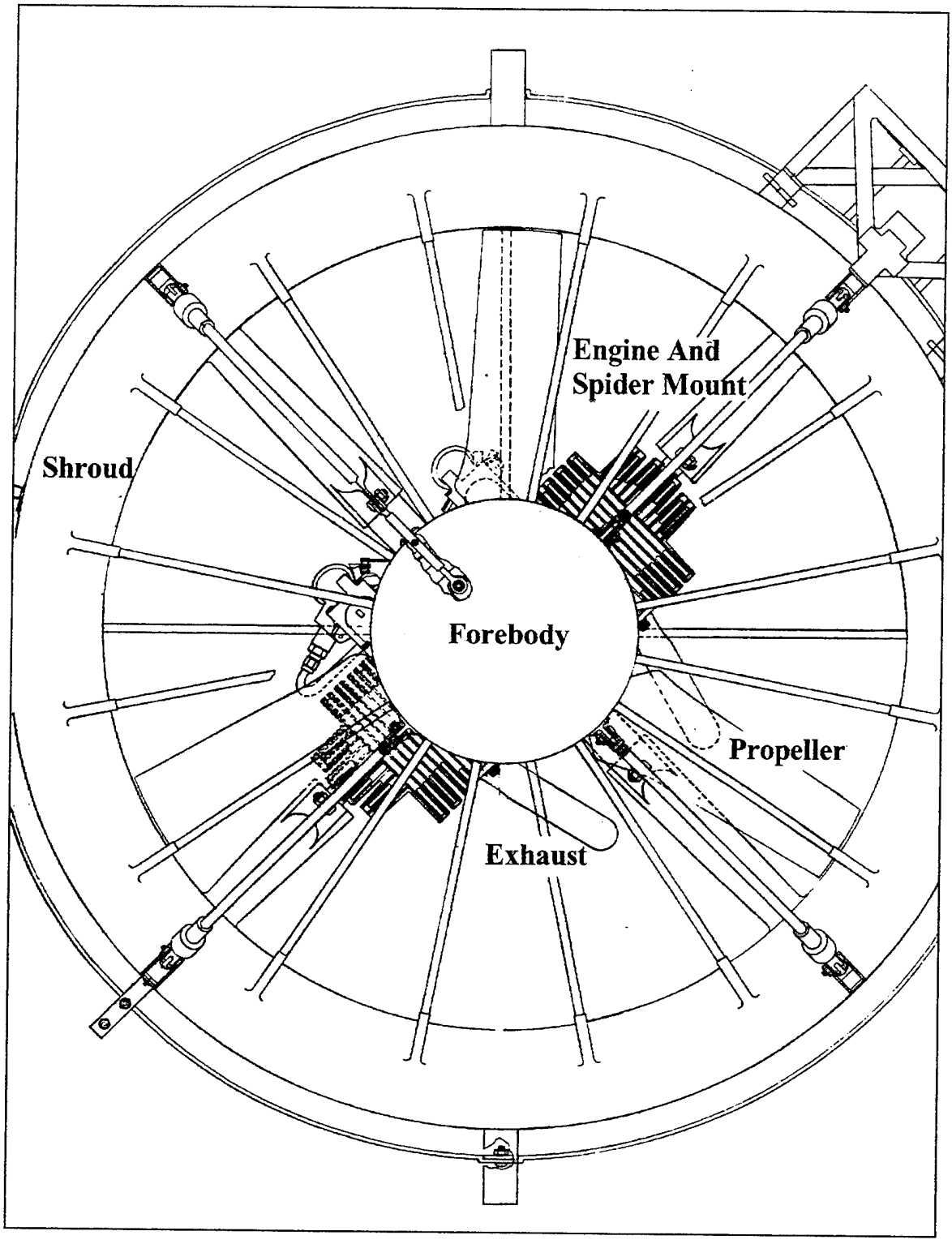

Figure A.2 - Top View of ADF and Engine [Ref. 15]

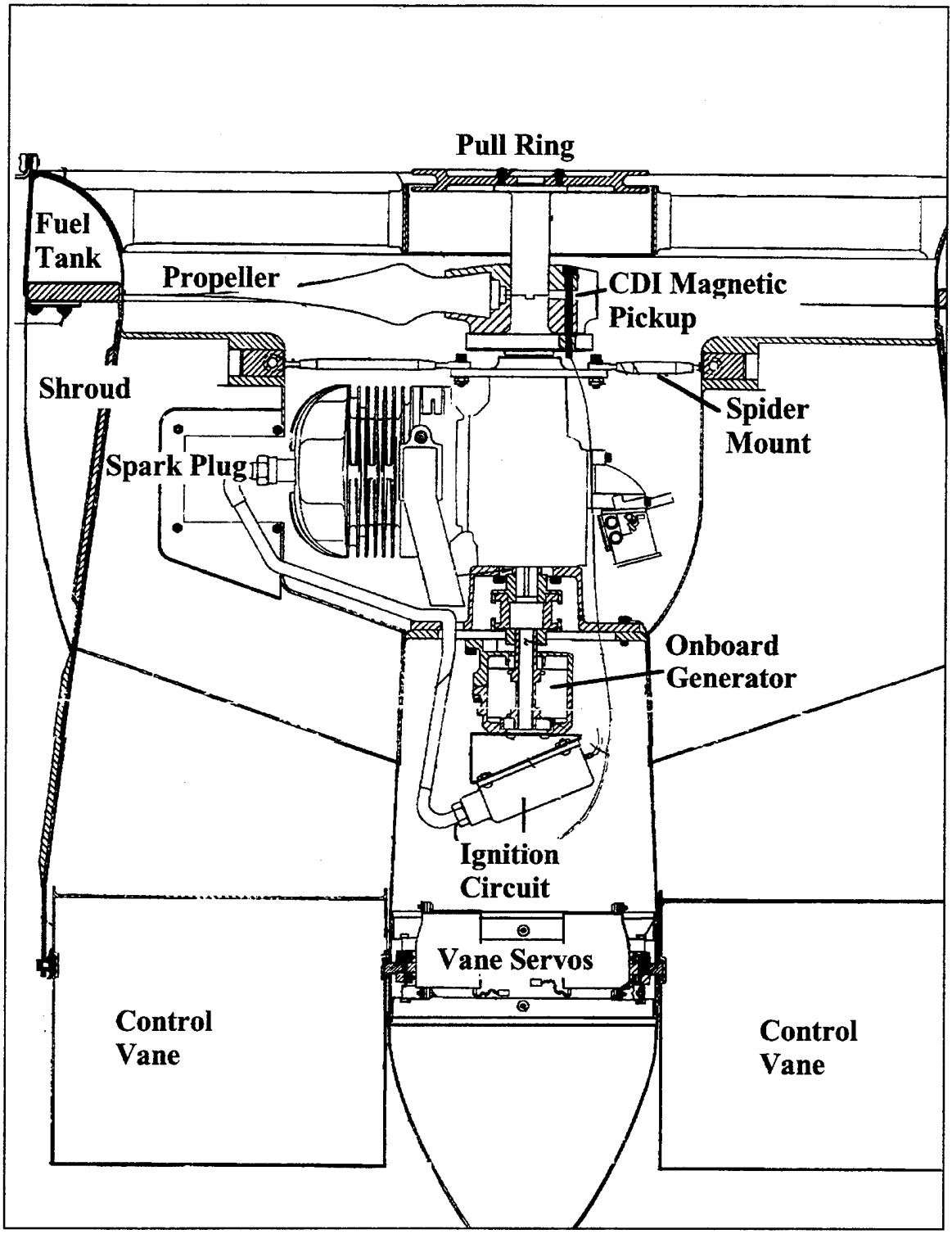

Figure A.3 - ADF Engine Side View [Ref. 15]

APPENDIX B: UPLINK HARDWARE

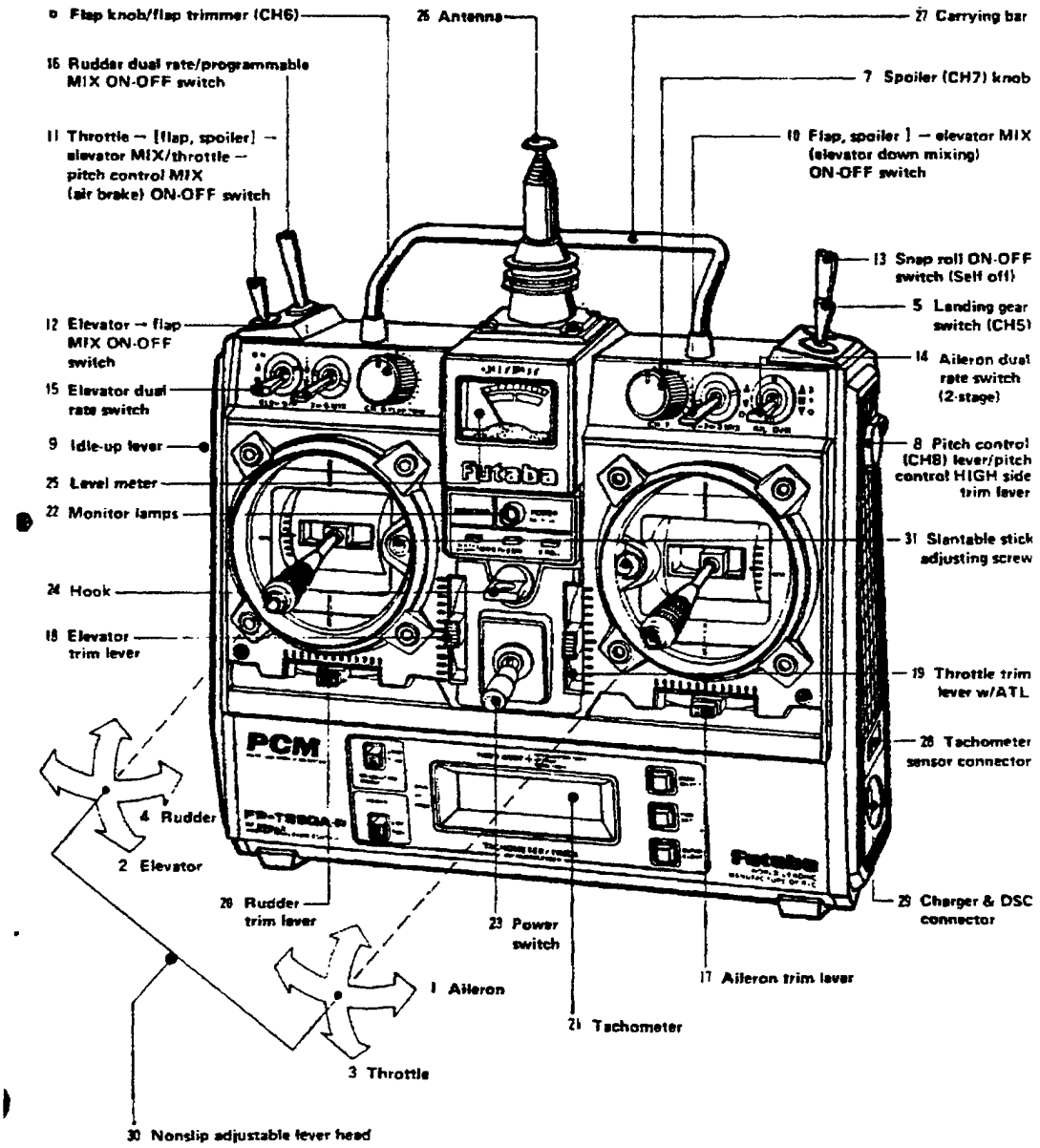

Figure B.1 - Transmitter [Ref. 22]

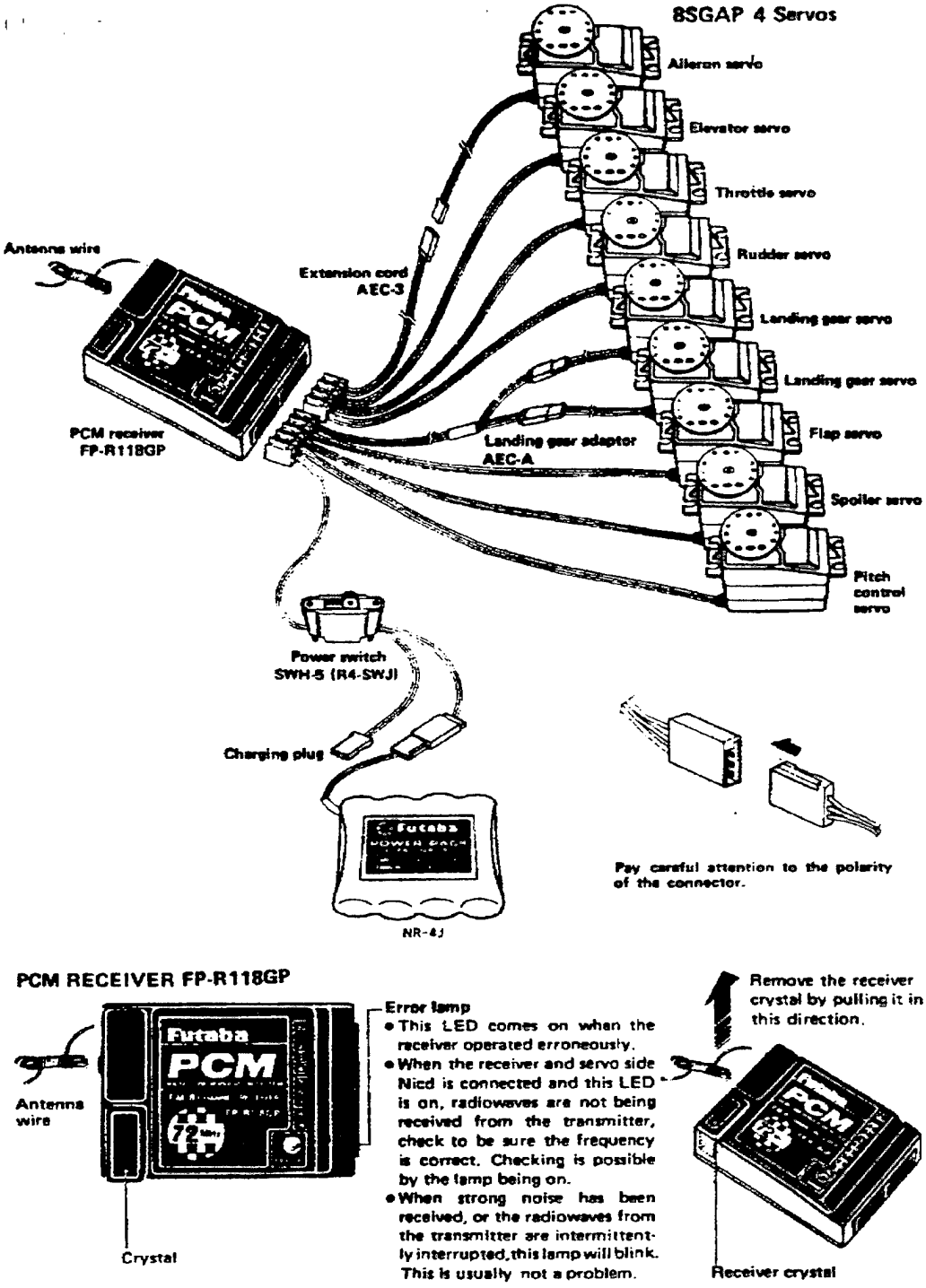

Figure B.2 - Receiver / Servo Connections [Ref. 22]

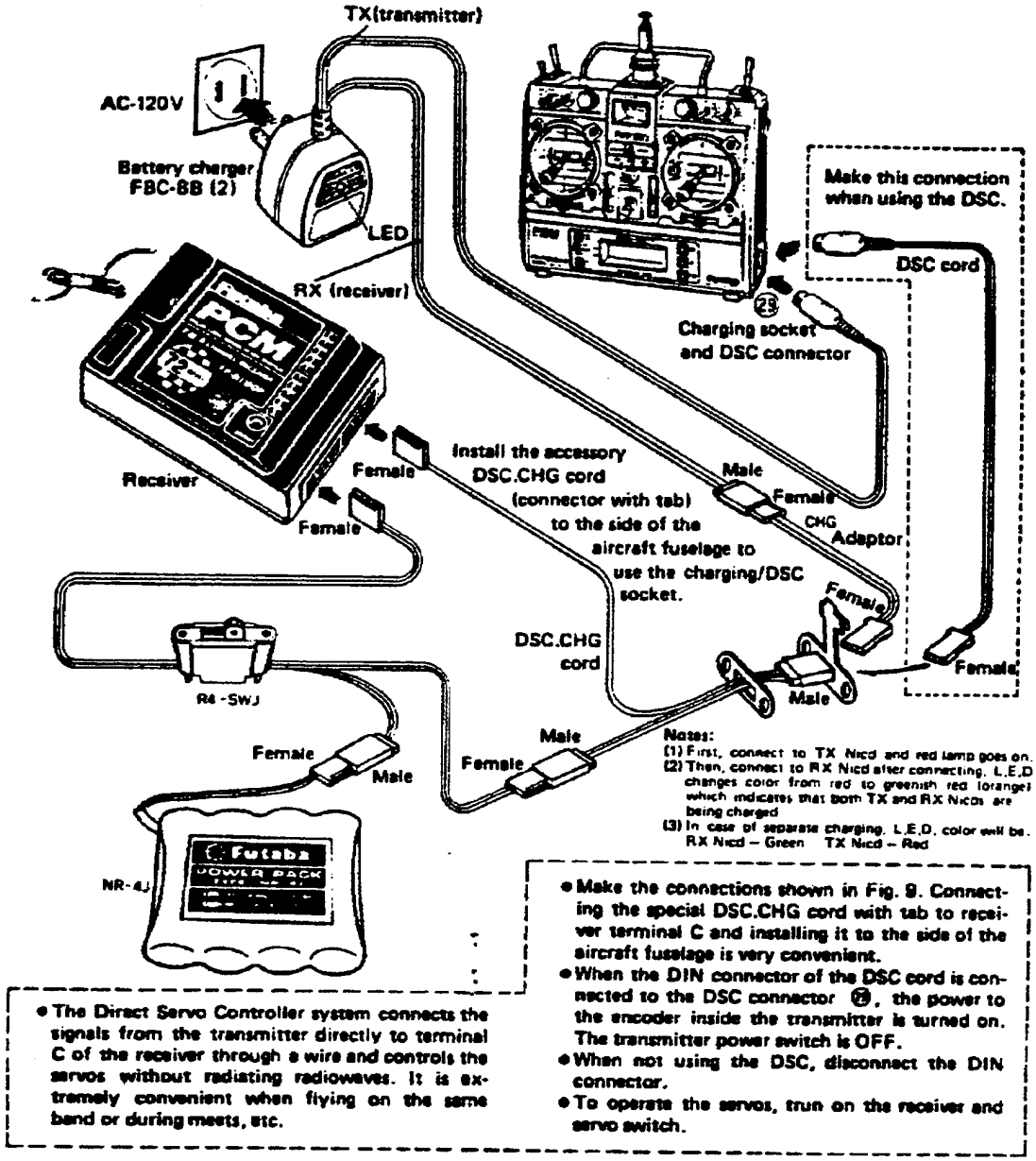

Figure B.3 - Battery Recharge [Ref. 22]

APPENDIX C: PERFORMANCE DATA

RPM And Thrust Data

Run #1			Run #2			Run #3		
ms	rpm	thrust	ms	rpm	thrust	ms	rpm	thrust
7.82	7672.634	116	7.64	7853.403	115	8.1	7407.407	121
7.9	7594.937	114	7.84	7653.061	114	8.18	7334.963	118
8.66	6928.406	105	8.44	7109.005	105	8.26	7263.923	119
9.84	6097.561	88	8.84	6787.33	90	8.86	6772.009	115
10.24	5859.375	68	10.46	5736.138	78	9.04	6637.168	113
11.12	5395.683	27	16.4	3658.537	27	9.06	6622.517	109
18.32	3275.109	25	18.08	3318.584	25	9.42	6369.427	90
						9.74	6160.164	92
						10.36	5791.506	78
						10.62	5649.718	66
						11.42	5253.94	62
						11.5	5217.391	56
						12.86	4665.63	44
						15.86	3783.102	24
						19.26	3115.265	14

Throttle Position And Thrust Data

	Thrust		
Throttle Position	Run # 1	Run # 2	Run # 3
0	21	25	25
17		27	27
25	67		
33		68	78
50	91	88	90
66		105	105
75	114		
83		114	114
100	121	116	115

APPENDIX D: FUEL USAGE AND TEMPERATURE DATA

Fuel And Rpm Data

Fuel Endurance Tests

Test # 1

Temp = 58 F
Press = 30.10 in

Beaker (full - 2000ml) = 5.90 lb
Beaker (Empty) = 2.58 lb
Fuel Weight = 3.32 lb

2000 ml = .528Gal

$$\frac{3.32\text{lb}}{.5283\text{Gal}} = 6.284 \text{ lb / Gal}$$

Run #	Desired Rpm	ms / rpm o-scope	Time (min)	Weight Before	Weight After	Fuel Used Ga	Endurance Gal/Hr
1	6000	9.96/6024	15	10.28	7.78	0.397836	1.591343
2	6000	10 / 6000	10	7.78	5.77	0.31986	1.91916
3	6000	9.94/6036	5	5.77	4.81	0.152769	1.833227

Test # 4

Temp =
Press =

Beaker (full - 2000ml) = 5.92 lb
Beaker (Empty) = 2.58
Fuel Weight (lb) = 3.34

2000 ml = .528Gal

$$\frac{3.34}{0.5233} = 6.322 \text{ lb / Gal}$$

Run #	Desired Rpm	ms / rpm o-scope	Time (min)	Weight Before	Weight After	Fuel Used Gal	Endurance Gal/Hr
10	5000	11.84/507	10	8.66	7.95	0.11298	0.677912
11	5500	11.1/5405	10	7.95	7.25	0.11139	0.668364
12	6500	9.17/6543	10	7.25	5.91	0.21324	1.27944
13	7000	8.6/6976	10	5.91	2.66	0.51718	3.103119

Test # 5

Temp = 78F
Press = 30.07

Beaker (full - 2000ml) = 5.88 lb
Beaker (Empty) = 2.58 lb
Fuel Weight (lb) =

2000 ml = .5283Gal

$\frac{3.3}{0.5233}$ = 6.246 lb / Gal

Run #	Desired Rpm	ms / rpm o-scope	Time (min)	Weight Before	Weight After	Fuel Used Gal	Endurance Gal/Hr
14	7500	7.96/7547	10	8.72	5.12	0.576	3.456
15	7200	8.27/7255	10	9.27	5.93	0.534	3.208
16	6800	8.81/6810	10	9.26	6	0.5219	3.13
17	6300	9.43/6362	7	7.21	5.73	0.2369	2.031
18	5800	10.29/583	10	8.48	7.21	0.2033	1.22

TEMPERATURE READINGS

Test # 1

Run # 1

Initial Temp = 58F

Alt = 30.10

Rpm = 6000

Minutes	Cyl Temp	Exhaust Temp
0		
1	320	682
2	327	680
3	328	689
4	327	687
5	332	696
6	331	695
7	330	697
8	330	702
9	330	698
10	330	700
11	331	697
12	332	699
13	328	702
14	331	701
15	331	701
16	244	237
17	232	209

Run # 2

Initial Temp = 58F

Alt = 30.10

Rpm = 6024

Minutes	Cyl Temp	Exhaust Temp
0	232	209
1	312	717
2	325	714
3	326	704
4	325	701
5	324	703
6	325	701
7	324	699
8	325	701
9	324	698
10	326	704

Run # 3

Initial Temp = 58F

Rpm = 5853

MInutes	Cyl Temp	Exhaust Temp
0	232	209
1	317	720
2	323	718
3	323	714
4	324	711
5	322	708

Test # 2
Run # 1

Initial Temp
= 78F
Alt = 30.07
Rpm = 5067

MInutes	Cyl Temp	Exhaust Temp
0	55	57
1	291	695
2	296	694
3	300	678
4	300	669
5	291	670
6	282	669
7	288	667
8	293	676
9	295	674
10	298	670

Test # 3
Run # 1

Initial Temp
= 78F
Alt = 30.07
Rpm = 5405

MInutes	Cyl Temp	Exhaust Temp
0	209	231
1	276	655
2	294	668
3	294	664
4	298	662
5	294	656
6	293	658
7	296	663
8	300	665
9	297	660
10	293	664

Test # 4
Run # 1

Initial Temp
= 78F
Alt = 30.07
Rpm = 6543

MInutes	Cyl Temp	Exhaust Temp
0	208	224
1	289	744
2	311	757
3	313	754
4	321	765
5	335	750
6	318	755
7	312	754
8	307	752
9	309	753
10	308	752

Test # 5
Run # 1

Initial Temp
= 78F
Alt = 30.07
Rpm = 6976

MInutes	Cyl Temp	Exhaust Temp
0	212	236
1	291	685
2	296	690
3	302	699
4	300	694
5	301	695
6	296	687
7	295	684
8	294	683
9	294	684
10	298	681

Test # 6

Run # 1

Initial Temp = 76F

Alt = 30.10

Rpm = 7537

MInutes	Cyl Temp	Exhaust Temp
0	282	260
1	287	677
2	287	677
3	288	675
4	289	674
5	290	675
6	292	675
7	286	676
8	288	676
9	290	674
10	289	676

Run # 2

Initial Temp = 76F

Alt = 30.10

Rpm = 7255

MInutes	Cyl Temp	Exhaust Temp
0	167	163
1	262	675
2	265	678
3	292	677
4	295	679
5	285	675
6	291	676
7	285	674
8	288	675
9	288	673
10	296	676

Run # 3

Initial Temp = 76F

Alt = 30.10

Rpm = 6810

MInutes	Cyl Temp	Exhaust Temp
0	216	171
1	265	686
2	285	680
3	287	676
4	285	680
5	285	681
6	284	679
7	281	676
8	287	691
9	290	691
10	291	693

Test # 7

Run # 1

Initial Temp = 68F

Alt = 30.08

Rpm = 5830

MInutes	Cyl Temp	Exhaust Temp
0	216	171
1	284	748
2	302	741
3	306	743
4	312	742
5	303	740
6	305	741
7	302	741
8	304	741
9	303	738
10	305	739

Run # 2

Initial Temp = 68F

Alt = 30.08

Rpm = 6362

MInutes	Cyl Temp	Exhaust Temp
0	170	215
1	287	710
2	294	707
3	289	706
4	293	704
5	294	711
6	297	711
7	295	705

APPENDIX E: CURVE FIT EQUATIONS

Figure	Description	Equation
14	Throttle Pos. Vs. Thrust	=21.25-0.40269*TP+0.10932*TP^2-0.0021907*TP^3+0.000017515*TP^4-0.000000051479*TP^5
15	Thrust Vs. RPM (Original)	=28-0.0129*RPM+0.00000335*RPM^2
15	Thrust Vs. RPM (New)	= -0.000000003253*RPM^3+0.000053454416*RPM^2 -0.255170625032*RPM+ 397.510986244515
19	Fuel Usage Vs. RPM	= -0.00000000015159*RPM^3+0.00000294677502*RPM^2 -0.0176389787831*RPM+ 34.0256458548718
20	Fuel Usage Vs. Thrust	=0.0004432323302*Thrust^2 -0.03269240885391*Thrust+1.07513175196086

LIST OF REFERENCES

1. Wagner, Williams, *Lightening Bugs and Other Reconnaissance Drones*, Aero Publishers, Inc., 1982.

2. *Short-Range Prototypes May Provide Core for Next Generation of UAV's*, AW&ST, December 9, 1991, p. 48.

3. *Short-Range Prototypes May Provide Core for Next Generation of UAV's*, AW&ST, December 9, 1991, p. 45.

4. *Air Force May Delay JPATS, TSSAM*, AW&ST, September 19,1994.

5. Kataras, Dimitris E., *Design And Implementation Of An Inertial Navigation System For Real Time Flight Of An Unmanned Air Vehicle*, Master's Thesis, Department of Aeronautics, Naval Postgraduate School, March, 1995.

6. E-Mail from David K. Costello to Issac Kaminer, July 8, 1994.

7. *Competitors Protest UAV Design Selection*, AW&ST, October 17, 1994.

8. *US. Military To Boost Tactical Recon in '95*, AW&ST, January 9,1995, p.22.

9. Munson, K., *World Unmanned Aircraft*, Jane's Publishing Co., London, 1988, p. 8.

10. *Optical Fibers Flies Hovering Robot*, Design News, March 27, I 989, p. 47.

11. Munson, K., *World Unmanned Aircraft*, Jane's Publishing Co., London, 1988, p. 58.

12. Bray, R.M., Lyons D.F. and Howard R.M., *Aerodynamics Analysis Of The Pioneer Unmanned Air Vehicle*, AIAA Paper 92-4635, AIAA Atmospheric Flight Mechanics Conference, Hilton Head, SC, 10-12 Aug. 1992.

13. Munson, K., *World Unmanned Aircraft*, Jane's Publishing Co. 1988, p. 9.

14. Stewart, John E. C., *Design of an Aquila Unmanned Air Vehicle*, Master's Thesis, Department of Aeronautics, Naval Postgraduate School, March, 1995.

15. Sandia National Laboratories, *Compilation of AROD Documents*, May 1988.

16. Moran, Patrick J., *Control Vane Guidance For A Ducted Fan Unmanned Air Vehicle*, Master's Thesis, Department of Aeronautics, Naval Postgraduate School, June, 1993.

17. Kress, Gregory, A., *Preliminary Development of a VTOL Unmanned Air Vehicle*, Master's Thesis, Department of Aeronautics, Naval Postgraduate School, September, 1992.

18. Stoney, Robert B., *Design, Fabrication and Test of a Vertical Attitude Takeoff and Landing Unmanned Air Vehicle*, Master's Thesis, Department of Aeronautics, Naval Postgraduate School, June, 1993.

19. Naval Air Warfare Center, Patuxent River, MD, *US. Naval Test Pilot School Flight Test Manual*, Veda Incorporated, September 30, 1992.

20. Beer and Johnston, *Mechanics of Materials*, McGraw-Hill, Inc., 1992.

21. Lindsey, G., "Class Notes For A 4 3202", Naval Postgraduate School, Monterey, CA.

22. Instructions And Operations Manual, Futaba Corporation, 1988, Irvine, CA.

INTTIAL DISTRIBUTION LIST

		No. Copies
1.	Defense Technical Information Center Cameron Station Alexandria, VA 22304-6145	2
2.	Library, Code 52 Naval Postgraduate School Monterey, CA 93 943 -510 I	2
3.	Chairman, Code AA Naval Postgraduate School Monterey, CA 93943-5000	1
4.	Professor Richard M. Howard, Code AA/Ho Naval Postgraduate School Monterey, CA 93943-5100	3
5.	Professor Issac I. Kaminer, Code AA/Ne Naval Postgraduate School Monterey, CA 93943-5 I 00	1
6.	Mr. Don Meeks, Code AA Naval Postgraduate School Monterey, CA 93943-5100	1
7.	LT Andrew L. Cibula Air Department USS Kitty Hawk (CV-63) FPO AP 96634-2770	1
8.	Mr. Joseph Cibula 270 Old Mill Rd. #60 Santa Barbara, CA 931	1
9.	Ms. Bettė Cibula 3164 Claymore Ln New Franken, WI 54229	1